Measuring superparticle masses at hadron collider using the transverse mass kink

Won Sang Cho[1], Kiwoon Choi[1],Yeong Gyun Kim[1,2], Chan Beom Park[1]

[1] *Department of Physics, KAIST, Daejon 305-701, Korea*
[2] *ARCSEC, Sejong University, Seoul 143-747, Korea*

Abstract

We present a detailed study of the collider observable m_{T2} applied for pair-produced superparticles decaying to visible particles and a pair of invisible lightest supersymmetric particles (LSPs). Analytic expressions of the maximum of m_{T2} over all events ($m_{T2}^{\max}$) are derived. It is noticed that if the decay product of each superparticle involves more than one visible particle, $m_{T2}^{\max}$ being a function of the *trial* LSP mass m_χ has a kink structure at $m_\chi =$ true LSP mass, which can be used to determine the mother superparticle mass and the LSP mass simultaneously. To see how well $m_{T2}^{\max}$ can be constructed from collider data, a Monte-Carlo analysis of the gluino m_{T2} is performed for some superparticle spectra.

1 Introduction

The Large Hadron Collider (LHC) at CERN will explore soon the TeV energy scale where new physics beyond the Standard Model (SM) is likely to reveal itself [1, 2]. Among various proposals, weak scale supersymmetry (SUSY) [3] is perhaps the most promising candidate for new physics at TeV as it provides a solution to the gauge hierarchy problem while complying with gauge coupling unification. Furthermore, with R-parity conservation, the lightest supersymmetric particle (LSP) becomes a natural candidate for the non-baryonic dark matter in the Universe.

Once SUSY signals are discovered through event excess beyond the SM backgrounds in inclusive search channels, the next step will be the measurement of SUSY particle masses and other physical properties through various exclusive decay chains [4]. Then, it might be possible to reconstruct the underlying SUSY theory, in particular the soft SUSY breaking terms, using the observed SUSY particle masses. In this regard, experimental information on gaugino masses can be particularly useful for distinguishing different SUSY breaking schemes as the theoretical predictions of low energy gaugino masses are quite robust compared to those on sfermion masses [5].

In a recent paper [6], we have examined the collider observable "gluino m_{T2} (stransverse mass)" which corresponds to the Cambridge m_{T2} variable [13, 14] applied to pair produced gluinos each of which is decaying to two quarks and one invisible neutralino LSP. Analytic expression of $m_{T2}^{\max}$ (= maximum of the gluino m_{T2} over all events) as a function of the *trial* LSP mass m_χ has been discussed with an observation that $m_{T2}^{\max}$ has a *kink structure*, i.e. a continuous but not differentiable cusp, at m_χ = true LSP mass, from which the gluino mass and the LSP mass can be determined simultaneously with good accuracy. If squarks are lighter than gluino, the gluino $m_{T2}^{\max}$ could determine the squark mass also. In this paper, we wish to provide a detailed discussion of m_{T2} in more general context, including the features which have been reported in [6][*].

This paper is organized as follows. In section 2, we discuss some generic properties of m_{T2}, and derive the analytic expression of $m_{T2}^{\max}$ for general symmetric decay of pair-produced mother superparticles. In section 3, we consider two specific processes, the decays of squark pair and of gluino pair, to examine the structure of m_{T2} in somewhat detail, and also perform a Monte Carlo LHC simulation for some superparticle spectra to examine how well can m_{T2} and $m_{T2}^{\max}$ be constructed from real collider data. Section 4 is devoted to the conclusion.

---

[*]After [6], the kink structure of the endpoint values of transverse mass observable has been discussed also in [7, 8]. For other approaches to measure superparticle masses at hadron collider, see [4, 9, 10, 11].

2 Generic features of m_{T2}

The kinematic variable 'transverse mass' (m_T) has been introduced to measure the W boson mass from the decay $W \to l\nu$ [12], for which the transverse mass is given by

$$m_T^2 = m_l^2 + m_\nu^2 + 2(E_T^l E_T^\nu - \mathbf{p}_T^l \cdot \mathbf{p}_T^\nu), \tag{1}$$

where m_l, m_ν and $\mathbf{p}_T^l, \mathbf{p}_T^\nu$ denote the mass and transverse momentum of the corresponding particle, respectively, and the transverse energies are defined as

$$E_T^l = \sqrt{|\mathbf{p}_T^l|^2 + m_l^2}, \quad E_T^\nu = \sqrt{|\mathbf{p}_T^\nu|^2 + m_\nu^2}. \tag{2}$$

On the other hand, the physical W mass is given by

$$\begin{aligned} m_W^2 &= m_l^2 + m_\nu^2 + 2p_l \cdot p_\nu \\ &= m_l^2 + m_\nu^2 + 2(E_T^l E_T^\nu \cosh \Delta\eta - \mathbf{p}_T^l \cdot \mathbf{p}_T^\nu) \geq m_T^2, \end{aligned} \tag{3}$$

where $\Delta\eta = \eta_l - \eta_\nu$ is the rapidity difference for a 4-momentum parameterized as

$$p^\mu = (E_T \cosh \eta, \mathbf{p}_T, E_T \sinh \eta).$$

Although the neutrino cannot be observed directly, its transverse momentum can be inferred from the measured total missing transverse momentum in event-by-event basis. Then, for each event, the transverse mass of W can be constructed from the observed values of $\mathbf{p}_T^l$ and $\mathbf{p}_T^\nu$, and an endpoint measurement of the m_T distribution determines the mother particle mass m_W:

$$m_W = \max_{\{\text{all events}\}} \left[m_T \right]. \tag{4}$$

More challenging situation for experimental measurement of unknown mother particle mass would be the case when there are more than one final state particles escaping the detection, so that the transverse momentum of each invisible particle can *not* be determined although the total missing transverse momentum is known. Additional difficulty would arise if the mass of the invisible daughter particle were not known in advance. Such situation is what one actually encounters in supersymmetric extension of the SM with conserved R-parity, in which superparticles are pair produced in collider experiment and each superparticle decay ends up with producing an invisible lightest supersymmetric particle (LSP) with unknown mass.

The m_{T2} variable [13, 14] which is sometimes called the "stransverse mass" is a generalization of the transverse mass to the case that a pair of massive mother particles are produced in hadron collider with a vanishing total transverse momentum in the laboratory frame, and subsequently decay to daughter particles including *two* invisible particles in

the final state[†]. In this paper, we will concentrate on the case that each mother particle decays into the same set of daughter particles, since such symmetric decay typically has higher event rate while showing the non-trivial structure which will be discussed in the following. Fig. 1 shows an example of such process in which mother superparticles were pair-produced and each of them decays into one neutralino LSP ($\tilde{\chi}_1^0$) and some visible particles. While the invisible part of each decay consists of only one particle (neutralino LSP), the visible part might contain one or more visible particle(s) in general.
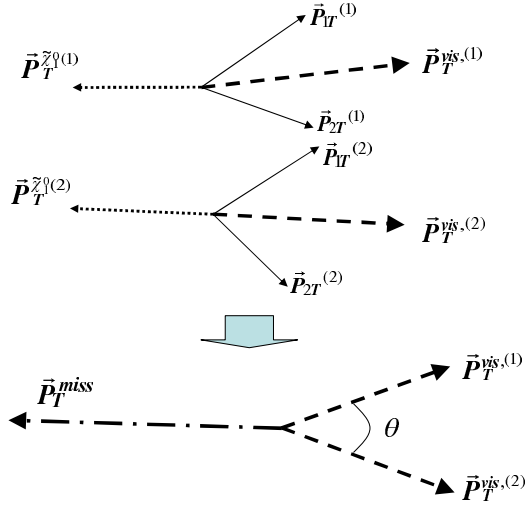

Figure 1: Kinematic situation for m_{T2} where $\mathbf{p}_T^{miss}$ denotes the total missing transverse momentum.

With two invisible LSPs in the final state, each LSP momentum can not be determined although the total missing transverse momentum $\mathbf{p}_T^{miss}$ can be measured experimentally. Furthermore, the LSP mass might not be known in advance. In such situation, one can introduce a *trial* LSP mass m_χ, and define the m_{T2} variable as follows [13, 14]:

$$m_{T2}(\mathbf{p}_T^{vis(1)}, m_{vis}^{(1)}, \mathbf{p}_T^{vis(2)}, m_{vis}^{(2)}, m_\chi) \equiv \min_{\{\mathbf{p}_T^{\chi(1)} + \mathbf{p}_T^{\chi(2)} = -\mathbf{p}_T^{vis(1)} - \mathbf{p}_T^{vis(2)}\}} \left[\max\{m_T^{(1)}, m_T^{(2)}\} \right], \quad (5)$$

where the minimization is performed over *trial* LSP momenta $\mathbf{p}_T^{\chi(i)}$ constrained as

$$\mathbf{p}_T^{\chi(1)} + \mathbf{p}_T^{\chi(2)} = \mathbf{p}_T^{miss},$$

[†]In Ref.[14], m_{T2} has been further generalized to the case involving more missing particles than two.

and $m_T^{(i)}$ $(i = 1, 2)$ denotes the transverse mass of the decay product of each initial mother particle:

$$m_T^{(i)} = \sqrt{(m_{vis}^{(i)})^2 + m_\chi^2 + 2(E_T^{vis(i)} E_T^{\chi(i)} - \mathbf{p}_T^{vis(i)} \cdot \mathbf{p}_T^{\chi(i)})}, \tag{6}$$

where $m_{vis}^{(i)}$ and $\mathbf{p}_T^{vis(i)}$ are the total invariant mass and the total transverse momentum of the visible part of each decay product:

$$
\begin{aligned}
\mathbf{p}_T^{vis(i)} &= \sum_\alpha \mathbf{p}_{\alpha T}, \\
(m_{vis}^{(i)})^2 &= \sum_\alpha m_\alpha^2 + 2 \sum_{\alpha > \beta} (E_\alpha E_\beta - \mathbf{p}_\alpha \cdot \mathbf{p}_\beta),
\end{aligned}
\tag{7}
$$

where $E_\alpha = \sqrt{m_\alpha^2 + |\mathbf{p}_\alpha|^2}$, $\mathbf{p}_\alpha$, and $\mathbf{p}_{\alpha T}$ denote the energy, momentum, and transverse momentum, respectively, of the α-th visible particle in the decay product of one mother particle, which are measured in the laboratory frame. Here, we ignore the initial state radiation effect, and then the total missing transverse momentum is given by

$$\mathbf{p}_T^{miss} = -(\mathbf{p}_T^{vis(1)} + \mathbf{p}_T^{vis(2)}), \tag{8}$$

and the transverse energies of the each visible system and of the LSP are defined as

$$E_T^{vis(i)} \equiv \sqrt{|\mathbf{p}_T^{vis(i)}|^2 + (m_{vis}^{(i)})^2}, \quad E_T^{\chi(i)} \equiv \sqrt{|\mathbf{p}_T^{\chi(i)}|^2 + m_\chi^2}. \tag{9}$$

In fact, one can consider also an m_{T2} with $m_{vis}^{(i)}$ replaced by the transverse mass of the visible part:

$$\left(m_T^{vis(i)}\right)^2 = \sum_\alpha m_\alpha^2 + 2 \sum_{\alpha > \beta} (E_{\alpha T} E_{\beta T} - \mathbf{p}_{\alpha T} \cdot \mathbf{p}_{\beta T}), \tag{10}$$

where $E_{\alpha T} = \sqrt{m_\alpha^2 + |\mathbf{p}_{\alpha T}|^2}$. Since $\mathbf{p}_T^{vis(i)}$ and $m_{vis}^{(i)}$ are treated as independent variables in the definition (5), once one finds the functional form of m_{T2} in terms of $\mathbf{p}_T^{vis(i)}$ and $m_{vis}^{(i)}$, the other m_{T2} defined in terms of $\mathbf{p}_T^{vis(i)}$ and $m_T^{vis(i)}$ can be easily obtained by replacing $m_{vis}^{(i)}$ with $m_T^{vis(i)}$.

Even without knowing the transverse momentum of each LSP, one can ensure that the true mother particle mass $\tilde{m}$ can *not* be smaller than m_{T2} when the trial LSP mass m_χ is chosen to be the true LSP mass $m_{\tilde{\chi}_1^0}$. This suggests that $\tilde{m}$ might be able to be determined by the endpoint value of m_{T2} distribution:

$$m_{T2}^{\max}(m_\chi) \equiv \max_{\{\text{all events}\}} \left[m_{T2}(\mathbf{p}_T^{vis(1)}, m_{vis}^{(1)}, \mathbf{p}_T^{vis(2)}, m_{vis}^{(2)}, m_\chi) \right] \tag{11}$$

4

which is a function of the trial LSP mass m_χ, satisfying

$$m_{T2}^{\max}(m_\chi = m_{\tilde{\chi}_1^0}) = \tilde{m} \equiv \text{mother particle mass.} \tag{12}$$

In order to see how m_{T2} is determined for a given event, let us first consider the minimization of m_T over unconstrained trial LSP momentum $\mathbf{p}_T^\chi$. Differentiating m_T^2 by $\mathbf{p}_T^\chi$, one finds

$$\frac{\partial m_T^2}{\partial \mathbf{p}_T^\chi} = 2\left(E_T^{vis}\frac{\mathbf{p}_T^\chi}{E_T^\chi} - \mathbf{p}_T^{vis}\right). \tag{13}$$

This implies that m_T has a stationary value when the trial LSP momentum satisfies

$$\mathbf{p}_T^\chi = \frac{E_T^\chi}{E_T^{vis}}\mathbf{p}_T^{vis} = \frac{m_\chi}{m_{vis}}\mathbf{p}_T^{vis}. \tag{14}$$

This stationary point actually corresponds to the global minimum of m_T for given values of m_{vis} and m_χ:

$$\left(m_T\right)_{\min} = m_T\big|_{\mathbf{p}_T^\chi/m_\chi = \mathbf{p}_T^{vis}/m_{vis}} = m_{vis} + m_\chi, \tag{15}$$

which is called the *unconstrained minimum* of the transverse mass [14].
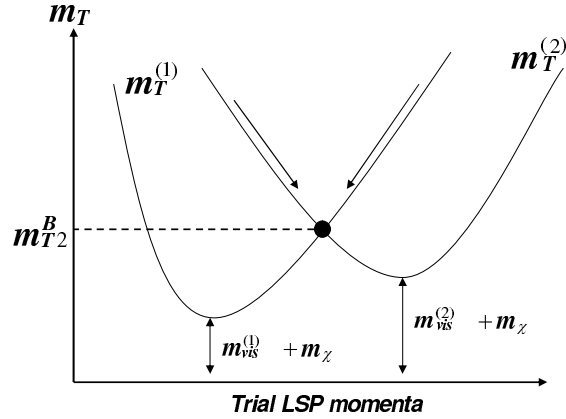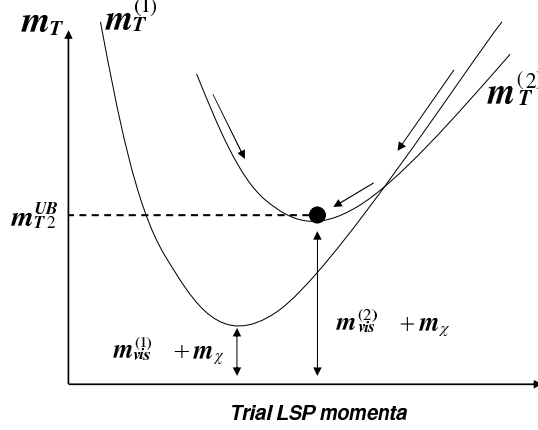

Figure 2: A balanced m_{T2} solution.

Figure 3: An unbalanced m_{T2} solution.

With the above observation, one can consider two different possibilities for how $m_T^{(i)}$ $(i = 1, 2)$ depend on trial LSP momenta, which are depicted in Fig. 2 and Fig. 3. The first possibility depicted in Fig. 2 is that $m_T^{(i)} \geq m_T^{(j)}$ for both i when the trial LSP transverse momenta take the value giving the unconstrained minimum of $m_T^{(j)}$ $(j \neq i)$, i.e.

$$
m_T^{(1)}\Big|_{\mathbf{p}_T^{\chi(1)} = -\mathbf{p}_T^{vis(1)} - \mathbf{p}_T^{vis(2)} - \tilde{\mathbf{p}}_T^{\chi(2)}} \geq m_T^{(2)}\Big|_{\mathbf{p}_T^{\chi(2)} = \tilde{\mathbf{p}}_T^{\chi(2)}} = m_{vis}^{(2)} + m_\chi,
$$

$$
m_T^{(2)}\Big|_{\mathbf{p}_T^{\chi(2)} = -\mathbf{p}_T^{vis(1)} - \mathbf{p}_T^{vis(2)} - \tilde{\mathbf{p}}_T^{\chi(1)}} \geq m_T^{(1)}\Big|_{\mathbf{p}_T^{\chi(1)} = \tilde{\mathbf{p}}_T^{\chi(1)}} = m_{vis}^{(1)} + m_\chi, \tag{16}
$$

where $\tilde{\mathbf{p}}_T^{\chi(i)}$ is the trial LSP transverse momentum giving the unconstrained minimum of $m_T^{(i)}$:

$$
\tilde{\mathbf{p}}_T^{\chi(i)} / m_\chi = \mathbf{p}_T^{vis(i)} / m_{vis}^{(i)}.
$$

In such case, the minimum of $\max\{m_T^{(1)}, m_T^{(2)}\}$ over possible trial LSP momenta is given by a *balanced m_{T2}* solution [14]

$$
m_{T2}^{\text{bal}} = \min_{\{\mathbf{p}_T^{\chi(1)} + \mathbf{p}_T^{\chi(2)} = -\mathbf{p}_T^{vis(1)} - \mathbf{p}_T^{vis(2)}, \, m_T^{(1)} = m_T^{(2)}\}} \left[m_T^{(1)} \right], \tag{17}
$$

where the minimization is performed over $\mathbf{p}_T^{\chi(i)}$ satisfying

$$
m_T^{(1)}(\mathbf{p}_T^{vis(1)}, \mathbf{p}_T^{\chi(1)}, m_{vis}^{(1)}, m_\chi) = m_T^{(2)}(\mathbf{p}_T^{vis(2)}, \mathbf{p}_T^{\chi(2)}, m_{vis}^{(2)}, m_\chi),
$$
$$
\mathbf{p}_T^{\chi(1)} + \mathbf{p}_T^{\chi(2)} = -\mathbf{p}_T^{vis(1)} - \mathbf{p}_T^{vis(2)}. \tag{18}
$$

6

The condition (16) might not be satisfied as in the case of Fig. 3 for which

$$m_T^{(1)}\big|_{\mathbf{p}_T^{\chi(1)}=-\mathbf{p}_T^{vis(1)}-\mathbf{p}_T^{vis(2)}-\tilde{\mathbf{p}}_T^{\chi(2)}} < m_T^{(2)}\big|_{\mathbf{p}_T^{\chi(2)}=\tilde{\mathbf{p}}_T^{\chi(2)}} = m_{vis}^{(2)} + m_\chi,$$ (19)

where $\tilde{\mathbf{p}}_T^{\chi(2)}$ is the trial LSP transverse momentum giving the unconstrained minimum of $m_T^{(2)}$. In such case, m_{T2} is obviously given by the unconstrained minimum of $m_T^{(2)}$. Solutions obtained in this way are called the *unbalanced* m_{T2} solution [14], and given by

$$m_{T2}^{\text{unbal}} = m_T^{(i)}\big|_{\mathbf{p}_T^{\chi(i)}/m_\chi=\mathbf{p}_T^{vis(i)}/m_{vis}^{(i)}} = m_{vis}^{(i)} + m_\chi \quad (i = 1 \text{ or } 2).$$ (20)

Note that unbalanced solution can accompany a balanced solution as Fig. 3 for which the crossing point of $m_T^{(1)}$ and $m_T^{(2)}$ corresponds to a balanced m_{T2} solution according to the definition (17). However obviously such balanced solution can *not* be a genuine m_{T2} defined as (5).

Recently, analytic expression of the balanced m_{T2} solution for generic event has been derived in Ref. [15], which we briefly recapitulate in the following. For this, let us rewrite $m_{T2}{}^{\ddagger}$ as

$$m_{T2}^2 = \min_{\substack{\beta_1+\beta_2=\sqrt{s}\Lambda-(\alpha_1+\alpha_2)\\ \beta_1^2=\beta_2^2=m_\chi^2}} \left[\max\{(\alpha_1+\beta_1)^2,(\alpha_2+\beta_2)^2\}\right],$$ (21)

where $V^2 = (V^0)^2 - \vec{V}\cdot\vec{V}$ is the scalar product of the $(1+2)$-dimensional momentum vector $V^\mu = (V^0, \vec{V})$, and the $(1+2)$-dimensional momenta $\alpha_i^\mu, \beta_i^\mu$ are given by

$$\alpha_1^\mu = (E_T^{vis(1)}, \mathbf{p}_T^{vis(1)}), \quad \alpha_2^\mu = (E_T^{vis(2)}, \mathbf{p}_T^{vis(2)}),$$
$$\beta_1^\mu = (E_T^{\chi(1)}, \mathbf{p}_T^{\chi(1)}), \quad \beta_2^\mu = (E_T^{\chi(2)}, \mathbf{p}_T^{\chi(2)}).$$ (22)

These momenta are related as

$$\alpha_1^\mu + \beta_1^\mu + \alpha_2^\mu + \beta_2^\mu = \sqrt{s}\,\Lambda^\mu = \sqrt{s}\,(1, 0, 0),$$ (23)

where $\sqrt{s}$ corresponds to the total transverse energy of the event. The square of the balanced m_{T2} solution corresponds to the minimum of $(\alpha_1+\beta_1)^2$ over all possible values of $\sqrt{s}$, subject to the following constraint:

$$\beta_1^2 = \beta_2^2 = m_\chi^2, \quad (\alpha_1+\beta_1)^2 = (\alpha_2+\beta_2)^2.$$ (24)

The procedure to obtain the balanced m_{T2} solution is first to solve (24) for β_1^μ and β_2^μ, and next minimize the resulting $(\alpha_1+\beta_1)^2$ over all allowed values of $\sqrt{s}$. Then, one finds

---

‡Throughout this paper, we ignore the initial state radiation, so the total missing transverse momentum is given by $\mathbf{p}_T^{miss} = -(\mathbf{p}_T^{vis(1)} + \mathbf{p}_T^{vis(2)})$.

[15]

$$\left(m_{T2}^{\text{bal}}\right)^2 = m_\chi^2 + A_T$$
$$+ \sqrt{\left(1 + \frac{4m_\chi^2}{2A_T - \left(m_{vis}^{(1)}\right)^2 - \left(m_{vis}^{(2)}\right)^2}\right)\left(A_T^2 - \left(m_{vis}^{(1)} m_{vis}^{(2)}\right)^2\right)}, \qquad (25)$$

where A_T is the Euclidean inner product of the two (1+2)-dimensional visible momenta α_1^μ and α_2^μ:

$$\begin{aligned} A_T &\equiv \alpha_1^0 \alpha_2^0 + \vec{\alpha_1} \cdot \vec{\alpha_2} \\ &= E_T^{vis(1)} E_T^{vis(2)} + \mathbf{p}_T^{vis(1)} \cdot \mathbf{p}_T^{vis(2)}, \end{aligned} \qquad (26)$$

and we have rewritten the result of [15] in a form convenient for our later discussion.

The m_{T2} solution obtained above has invariance properties which will be useful for the derivation of the possible range of m_{T2}. First of all, the transverse masses $m_T^{(i)}$ and thus m_{T2} are invariant under arbitrary *independent longitudinal Lorentz boost* of each mother particle in the pair, which is obviously true as both E_T and $\mathbf{p}_T$ are invariant under longitudinal boost. Furthermore, m_{T2} is invariant also under the following transformation of the $(1+2)$-dimensional momenta $\alpha_i^\mu = (E_T^{vis(i)}, \mathbf{p}_T^{vis(i)})$ and $\beta_i^\mu = (E_T^{\chi(i)}, \mathbf{p}_T^{\chi(i)})$:

$$\begin{aligned} \alpha_1^\mu &\to \Lambda_\nu^\mu(\vec{v})\alpha_1^\nu, \quad \beta_1^\mu \to \Lambda_\nu^\mu(\vec{v})\beta_1^\nu, \\ \alpha_2^\mu &\to \Lambda_\nu^\mu(-\vec{v})\alpha_2^\nu, \quad \beta_2^\mu \to \Lambda_\nu^\mu(-\vec{v})\beta_2^\nu, \end{aligned} \qquad (27)$$

where $\Lambda_\nu^\mu(\vec{v})$ denotes the (1+2)-dimensional Lorentz transformation matrix for 2-dimensional boost parameter $\vec{v}$. The condition (16) and the relation (18) are covariant under the above transformation, i.e. if (16) or (18) is satisfied by some $(1+2)$-dimensional momenta, it is satisfied also by the transformed momenta. (In appendix A, we provide a more detailed discussion on the covariance of (16) and (19) under the transformation (27).) As the transverse mass itself is obviously invariant, this means that the balanced solution m_{T2}^{bal} defined as (17) is invariant under the transformation (27), which can be confirmed also by the explicit solution (25). As for the unbalanced solution, (14) and (19) are covariant, so the unbalanced solution m_{T2}^{unbal} defined as (20) is invariant also.

In fact, for generic $\mathbf{p}^{vis(i)}$, the transformation (27) of the $(1+2)$-dimensional vector $(E_T, \mathbf{p}_T)$ does *not* have a direct connection to a true Lorentz transformation of the 4-momentum $(E, \mathbf{p})$. However, if both $\mathbf{p}^{vis(1)}$ and $\mathbf{p}^{vis(2)}$ are in transverse direction, it can be identified as a true Lorentz transformation corresponding to *a back-to-back boost of the mother particle pair in transverse direction*. We thus conclude that m_{T2} for visible momenta satisfying $\mathbf{p}^{vis(i)} = \mathbf{p}_T^{vis(i)}$ $(i = 1, 2)$ is invariant under a back-to-back boost of the mother particle pair in the direction along the transverse plane T.

Let us now examine the possible range of m_{T2}, in particular its maximal value. Our starting point is the following theorem which will be proved in appendix A: m_{T2} of any event induced by mother particle pair having a vanishing total transverse momentum in the laboratory frame is *bounded above* by another m_{T2} of an event induced by mother particle pair *at rest*. More explicitly, for generic $\mathbf{p}^{vis(i)}$ measured in the laboratory frame,

$$m_{T2}(\mathbf{p}_T^{vis(i)}, m_{vis}^{(i)}, m_\chi) \leq m_{T'2}(\mathbf{q}^{vis(i)}, m_{vis}^{(i)}, m_\chi), \tag{28}$$

where $\mathbf{q}^{vis(i)}$ is the Lorentz boost of $\mathbf{p}^{vis(i)}$ to the rest frame of the i-th mother particle, T' is the plane spanned by $\mathbf{q}^{vis(1)}$ and $\mathbf{q}^{vis(2)}$, so $\mathbf{q}^{vis(i)} = \mathbf{q}_{T'}^{vis(i)}$ by definition, and the equality in the above bound holds when $T = T'$. Note that T is a fixed transverse plane which is independent of the event momenta, while T' varies following the rest frame momenta $\mathbf{q}^{vis(i)}$.

By definition, $\mathbf{q}^{vis(i)}$ corresponds to the total visible momentum for the decay of the i-th mother particle, $\Phi_i \to \text{visibles} + \tilde{\chi}_1^0$, measured in the rest frame of Φ_i, and thus its magnitude is uniquely fixed by the mother particle mass $\tilde{m}$, the invariant mass $m_{vis}^{(i)}$ of the visible part, and the true LSP mass $m_{\tilde{\chi}_1^0}$:

$$|\mathbf{q}^{vis(i)}| \;=\; \frac{1}{2\tilde{m}} \left[\left((\tilde{m} + m_{vis}^{(i)})^2 - m_{\tilde{\chi}_1^0}^2 \right) \left((\tilde{m} - m_{vis}^{(i)})^2 - m_{\tilde{\chi}_1^0}^2 \right) \right]^{1/2}. \tag{29}$$

As a consequence, $m_{T'2}$ can be described by the three event variables, $m_{vis}^{(1)}, m_{vis}^{(2)}$ and θ, where θ is the angle between $\mathbf{q}^{vis(1)}$ and $\mathbf{q}^{vis(2)}$:

$$m_{T'2}(\mathbf{q}^{vis(i)}, m_{vis}^{(i)}, m_\chi) \equiv \mathcal{F}(m_{vis}^{(i)}, \theta, m_\chi). \tag{30}$$

Combined with (28), this leads to

$$
\begin{aligned}
m_{T2}^{\max}(m_\chi) &\equiv \max_{\{\text{all events in the lab frame}\}} \left[m_{T2}(\mathbf{p}_T^{vis(i)}, m_{vis}^{(i)}, m_\chi) \right] \\
&\leq \max_{\{m_{vis}^{(i)}, \theta\}} \left[\mathcal{F}(m_{vis}^{(i)}, \theta, m_\chi) \right] \equiv \mathcal{F}^{\max}(m_\chi).
\end{aligned} \tag{31}
$$

It is always a possible event that both $\mathbf{q}^{vis(1)}$ and $\mathbf{q}^{vis(2)}$ are along the direction of the transverse plane T, i.e. $T' = T$. For such event, the invariance of m_{T2} under longitudinal and back-to-back transverse boosts implies

$$m_{T2}(\mathbf{q}_T^{vis(i)}, m_{vis}^{(i)}, m_\chi) = m_{T2}(\mathbf{p}_T^{vis(i)}, m_{vis}^{(i)}, m_\chi) \tag{32}$$

where now $\mathbf{p}^{vis(i)}$ are the momenta obtained by arbitrary back-to-back transverse boost along $T = T'$ and subsequent arbitrary longitudinal boost starting from $\mathbf{q}^{vis(i)}$. For any $\mathbf{q}^{vis(i)}$, one can choose an appropriate boost for which $\mathbf{p}^{vis(i)}$ correspond to the visible momenta of some event observed in the laboratory frame. This means that for any $\mathbf{q}^{vis(i)}$,

there exist some laboratory events whose m_{T2} is same as the corresponding $\mathcal{F}(m_{vis}^{(i)}, \theta, m_\chi)$, therefore the bound (31) actually corresponds to an identity as

$$m_{T2}^{\max}(m_\chi) = \mathcal{F}^{\max}(m_\chi). \tag{33}$$

In appendix B, we will show

$$\frac{\partial \mathcal{F}}{\partial \theta} \leq 0 \quad \text{for any } m_{vis}^{(i)}, m_\chi, \text{ and } 0 \leq \theta \leq \pi,$$

$$\left. \frac{\partial \mathcal{F}}{\partial m_{vis}^{(i)}} \right|_{\theta=0} = \begin{cases} \leq 0 & \text{for } m_\chi < m_{\tilde{\chi}_1^0} \text{ and any } m_{vis}^{(i)} \\ \geq 0 & \text{for } m_\chi > m_{\tilde{\chi}_1^0} \text{ and any } m_{vis}^{(i)}, \end{cases} \tag{34}$$

and thus the global maximum of $\mathcal{F}$ over the full 3-dimensional event space of $\{m_{vis}^{(i)}, \theta\}$ is given by

$$\mathcal{F}^{\max}(m_\chi) = \begin{cases} \mathcal{F}_<^{\max} & \text{for } m_\chi < m_{\tilde{\chi}_1^0} \\ \mathcal{F}_>^{\max} & \text{for } m_\chi > m_{\tilde{\chi}_1^0}, \end{cases} \tag{35}$$

where

$$\begin{aligned}
\mathcal{F}_<^{\max} &= \mathcal{F}(m_{vis}^{(1)} = m_{vis}^{\min}, m_{vis}^{(2)} = m_{vis}^{\min}, \theta = 0, m_\chi), \\
\mathcal{F}_>^{\max} &= \mathcal{F}(m_{vis}^{(1)} = m_{vis}^{\max}, m_{vis}^{(2)} = m_{vis}^{\max}, \theta = 0, m_\chi)
\end{aligned} \tag{36}$$

with

$$m_{vis}^{\min} \leq m_{vis}^{(i)} \leq m_{vis}^{\max}. \tag{37}$$

In this section, for simplicity we limit ourselves to the one-dimensional event space with $m_{vis}^{(1)} = m_{vis}^{(2)}$ and $\theta = 0$, while leaving the discussion of full event space in appendix B.

For $m_{vis}^{(1)} = m_{vis}^{(2)}$, the unconstrained minima of $m_T^{(i)}$ have the same value, so m_{T2} is always obtained as a balanced solution. One can then use the balanced solution (25) for $\mathbf{p}^{vis(i)} = \mathbf{q}^{vis(i)}$ to find

$$\begin{aligned}
\tilde{\mathcal{F}}(m_{vis}, m_\chi) &\equiv \mathcal{F}(m_{vis}^{(1)} = m_{vis}, m_{vis}^{(2)} = m_{vis}, \theta = 0, m_\chi) \\
&= \frac{\tilde{m}^2 + m_{vis}^2 - m_{\tilde{\chi}_1^0}^2}{2\tilde{m}} + \frac{\left[\left(\tilde{m}^2 - m_{vis}^2 + m_{\tilde{\chi}_1^0}^2 \right)^2 + 4\tilde{m}^2 \left(m_\chi^2 - m_{\tilde{\chi}_1^0}^2 \right) \right]^{1/2}}{2\tilde{m}}
\end{aligned} \tag{38}$$

where $\tilde{m}$ is the mother particle mass, $m_{\tilde{\chi}_1^0}$ is the true LSP mass, and we have used (29) for $|\mathbf{q}^{vis(i)}|$. Note that $\tilde{\mathcal{F}}(m_{vis}, m_\chi = m_{\tilde{\chi}_1^0}) = \tilde{m}$, and thus $m_{T2}^{\max}(m_\chi = m_{\tilde{\chi}_1^0}) = \tilde{m}$ as required.

The function $\tilde{\mathcal{F}}(m_{vis}, m_\chi)$ has an interesting feature. From

$$\frac{\partial \tilde{\mathcal{F}}}{\partial m_{vis}} = \frac{m_{vis}}{\tilde{m}} \left(1 - \frac{\tilde{m}^2 + m_{\tilde{\chi}_1^0}^2 - (m_{vis})^2}{\sqrt{(\tilde{m}^2 + m_{\tilde{\chi}_1^0}^2 - (m_{vis})^2)^2 + 4\tilde{m}^2(m_\chi^2 - m_{\tilde{\chi}_1^0}^2)}} \right), \tag{39}$$

10

one easily finds

$$\frac{\partial \tilde{\mathcal{F}}}{\partial m_{vis}} = \begin{cases} \leq 0 & \text{if} \ \ m_\chi < m_{\tilde{\chi}_1^0} \\ \geq 0 & \text{if} \ \ m_\chi > m_{\tilde{\chi}_1^0}. \end{cases} \tag{40}$$

This corresponds to the special limit of the general result (34), and yields

$$m_{T2}^{\max}(m_\chi) = \begin{cases} \mathcal{F}_<^{\max}(m_\chi) = \tilde{\mathcal{F}}(m_{vis} = m_{vis}^{\min}, m_\chi) & \text{if} \ \ m_\chi < m_{\tilde{\chi}_1^0}, \\ \mathcal{F}_>^{\max}(m_\chi) = \tilde{\mathcal{F}}(m_{vis} = m_{vis}^{\max}, m_\chi) & \text{if} \ \ m_\chi > m_{\tilde{\chi}_1^0}. \end{cases} \tag{41}$$

In the above, we have obtained $m_{T2}^{\max}$ from the balanced solution for $m_{vis}^{(1)} = m_{vis}^{(2)}$. However, this does not mean that $m_{T2}^{\max}$ is obtained only by the balanced solution. As we will see in the next section, $m_{T2}^{\max}$ for $m_\chi > m_{\tilde{\chi}_1^0}$ can be obtained also by unbalanced m_{T2} solution. In some of such case, the balanced solution giving $m_{T2}^{\max}$ has $\mathbf{p}_T^{miss} = 0$, and thus is eliminated by the event selection imposing a nonzero lower bound on $|\mathbf{p}_T^{miss}|$ when one constructs $m_{T2}^{\max}$ from collider data. On the other hand, the unbalanced solution giving $m_{T2}^{\max}$ has a large $\mathbf{p}_T^{miss}$, so plays an crucial role for the construction of $m_{T2}^{\max}$ from collider data.

If the decay product of each mother particle contains only one visible particle ψ, then m_{vis} is fixed to be m_ψ, and $m_{T2}^{\max}$ is given by

$$m_{T2}^{\max}(m_\chi) = \tilde{\mathcal{F}}(m_{vis} = m_\psi, m_\chi)$$
$$= \frac{\tilde{m}^2 + m_\psi^2 - m_{\tilde{\chi}_1^0}^2}{2\tilde{m}} + \frac{\left[\left(\tilde{m}^2 - m_\psi^2 + m_{\tilde{\chi}_1^0}^2 \right)^2 + 4\tilde{m}^2 \left(m_\chi^2 - m_{\tilde{\chi}_1^0}^2 \right) \right]^{1/2}}{2\tilde{m}}. \tag{42}$$

Usually ψ is much lighter than the LSP, so one can take the approximation $m_\psi \simeq 0$, for which

$$m_{T2}^{\max}(m_\chi) = \frac{\tilde{m}^2 - m_{\tilde{\chi}_1^0}^2}{2\tilde{m}} + \sqrt{\left(\frac{\tilde{m}^2 - m_{\tilde{\chi}_1^0}^2}{2\tilde{m}} \right)^2 + m_\chi^2}. \tag{43}$$

A simple example giving this form of $m_{T2}^{\max}$ would be the squark pair decay[§], $\tilde{q}\tilde{q} \rightarrow q\tilde{\chi}_1^0 q\tilde{\chi}_1^0$, whose m_{T2} will be discussed in more detail in the next section.

If the decay product of each mother particle contains more than one visible particles, $m_{T2}^{\max}$ has an interesting feature which was first noticed in [6]. In such case, m_{vis} can vary from $m_{vis}^{\min}$ to $m_{vis}^{\max}$, and so $m_{T2}^{\max}(m_\chi)$ at $m_\chi > m_{\tilde{\chi}_1^0}$ takes a *different* functional form from the one at $m_\chi < m_{\tilde{\chi}_1^0}$. As a consequence, $m_{T2}^{\max}$ has a *kink structure*, i.e. a continuous but not differentiable cusp, at $m_\chi = m_{\tilde{\chi}_1^0}$:

$$\frac{(d\mathcal{F}_>^{\max}/dm_\chi)_{m_\chi=m_{\tilde{\chi}_1^0}}}{(d\mathcal{F}_<^{\max}/dm_\chi)_{m_\chi=m_{\tilde{\chi}_1^0}}} = 1 + \frac{(m_{vis}^{\max})^2 - (m_{vis}^{\min})^2}{\tilde{m}^2 + m_{\tilde{\chi}_1^0}^2 - (m_{vis}^{\max})^2} > 1, \tag{44}$$

[§]Throughout this paper, we do not distinguish squark from anti-squark as we are considering only the kinematics.

11

which becomes sharper when $m_{vis}^{\max}$ becomes larger for a given value of $m_{vis}^{\min}$.

If visible particles in the decay product are much lighter than LSP, one can set $m_{vis}^{\min} \simeq 0$, and then

$$
\begin{aligned}
\mathcal{F}_<^{\max}(m_\chi) &= \tilde{\mathcal{F}}(m_{vis} = 0, m_\chi) \\
&= \frac{\tilde{m}^2 - m_{\tilde{\chi}_1^0}^2}{2\tilde{m}} + \sqrt{\left(\frac{\tilde{m}^2 - m_{\tilde{\chi}_1^0}^2}{2\tilde{m}}\right)^2 + m_\chi^2}.
\end{aligned}
\tag{45}
$$

On the other hand, even for a given number of visible particles in the final state, $m_{T2}^{\max}$ can have a different value depending upon the intermediate stage of the decay process. If the decay process $\Phi_i \to$ visibles $+ \tilde{\chi}_1^0$ does not involve any intermediate on-shell particle lighter than the mother particle Φ_i, one finds

$$
m_{vis}^{\max} = \tilde{m} - m_{\tilde{\chi}_1^0},
\tag{46}
$$

which results in

$$
\mathcal{F}_>^{\max}(m_\chi) = m_\chi + \left(\tilde{m} - m_{\tilde{\chi}_1^0}\right).
\tag{47}
$$

However, if visible particles are produced by a chain of decay processes involving intermediate on-shell particle(s), $m_{vis}^{\max}$ has a smaller value. For instance, if the decay chain involves one intermediate on-shell particle ϕ with $m_\phi < \tilde{m}$, e.g. $\Phi_i \to \phi +$ visible $\to \tilde{\chi}_1^0 +$ more visibles, the maximal value of $m_{vis}^{(i)}$ for the final state is given by

$$
m_{vis}^{\max} = \frac{\sqrt{(\tilde{m}^2 - m_\phi^2)(m_\phi^2 - m_{\tilde{\chi}_1^0}^2)}}{m_\phi},
\tag{48}
$$

for which

$$
\begin{aligned}
\mathcal{F}_>^{\max}(m_\chi) &= \left(\frac{\tilde{m}}{2}(1 - \frac{m_\phi^2}{\tilde{m}^2}) + \frac{\tilde{m}}{2}(1 - \frac{m_{\tilde{\chi}_1^0}^2}{m_\phi^2})\right) \\
&\quad + \sqrt{\left(\frac{\tilde{m}}{2}(1 - \frac{m_\phi^2}{\tilde{m}^2}) - \frac{\tilde{m}}{2}(1 - \frac{m_{\tilde{\chi}_1^0}^2}{m_\phi^2})\right)^2 + m_\chi^2}.
\end{aligned}
\tag{49}
$$

In Fig. 4, we depict the behavior of $m_{T2}^{\max}(m_\chi)$ for the case without any intermediate on-shell particle ($m_\phi > \tilde{m}$) and also the case of decay chain involving an intermediate on-shell particle ($m_\phi < \tilde{m}$). As the value of $m_{vis}^{\max}$ for the case without intermediate on-shell particle is bigger than the value of $m_{vis}^{\max}$ for the other case, the kink structure of Fig. 4(a) is sharper than that of Fig. 4(b) as anticipated in (44). A simple example of the process that each mother particle is producing more than one visible particles is the gluino pair decay: $\tilde{g}\tilde{g} \to q q \tilde{\chi}_1^0 q q \tilde{\chi}_1^0$, whose m_{T2} will be discussed in more detail in the next section.
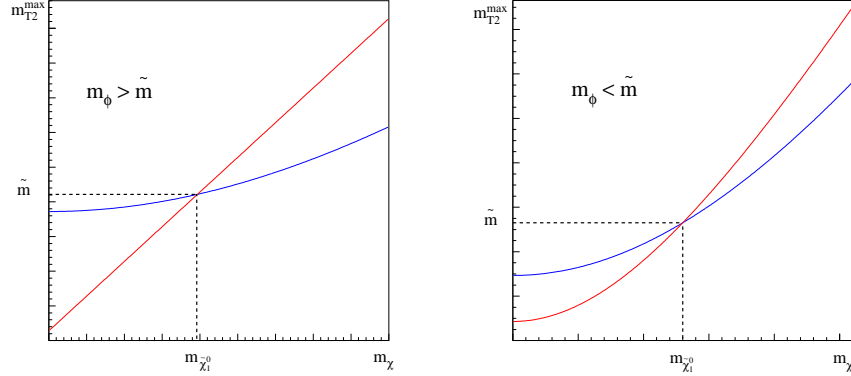
12

Figure 4: $m_{T2}^{\max}$ for (a) $m_\phi > \tilde{m}$, (b) $m_\phi < \tilde{m}$

3   Features of squark and gluino m_{T2}

In this section, we discuss in more detail the m_{T2} of two specific processes, the decay of pair-produced squarks, $\tilde{q}\tilde{q} \to q\tilde{\chi}_1^0 q\tilde{\chi}_1^0$, as an example of the case that each mother particle decays to one visible particle and one invisible LSP, and the decay of pair-produced gluinos, $\tilde{g}\tilde{g} \to qq\tilde{\chi}_1^0 qq\tilde{\chi}_1^0$, as an example of the next case that the decay product of each mother particle contains more than one visible particle. We also perform a Monte Carlo LHC simulation for some superparticle spectra to examine how well can m_{T2} and $m_{T2}^{\max}$ be constructed from real collider data.

3.1   Squark m_{T2}

Let us consider m_{T2} for the process in which a pair of squarks are produced in proton-proton collision and each squark decays subsequently into one quark and one LSP:

$$pp \to \tilde{q}\tilde{q} \to q\tilde{\chi}_1^0 q\tilde{\chi}_1^0, \tag{50}$$

where q denotes the 1st or 2nd generation quark. A characteristic feature of this process is that $m_{vis}^{(1)} = m_{vis}^{(2)} = m_q$, and thus $m_T^{(1)}$ and $m_T^{(2)}$ have the same unconstrained minimum:

$$\left(m_T^{(1)}\right)_{\min} = \left(m_T^{(2)}\right)_{\min} = m_\chi + m_q. \tag{51}$$

Then, m_{T2} is always obtained as a balanced solution as shown in Fig. 2, and the resulting balanced solution (25) is simplified as

$$m_{T2}^2 \;=\; m_\chi^2 + A_T + \sqrt{\left(A_T - m_q^2 + 2m_\chi^2\right)\left(A_T + m_q^2\right)}, \tag{52}$$

13

giving

$$m_{T2} = \sqrt{\frac{A_T + m_q^2}{2}} + \sqrt{\frac{A_T - m_q^2 + 2m_\chi^2}{2}}, \tag{53}$$

where

$$
\begin{aligned}
A_T &\equiv E_T^{vis(1)} E_T^{vis(2)} + \mathbf{p}_T^{vis(1)} \cdot \mathbf{p}_T^{vis(1)} \\
&= E_T^{vis(1)} E_T^{vis(2)} + |\mathbf{p}_T^{vis(1)}||\mathbf{p}_T^{vis(2)}| \cos\theta
\end{aligned} \tag{54}
$$

for $E_T^{vis(i)} = \sqrt{|\mathbf{p}_T^{vis(i)}|^2 + m_q^2}$ $(i = 1, 2)$.

As was discussed in the previous section, m_{T2} of any event induced by mother particle pair having a vanishing total transverse momentum in the laboratory frame is bounded above by another m_{T2} of an event induced by mother particle pair at rest. For a squark pair at rest, the magnitude of quark momentum from each squark decay is given by

$$|\mathbf{p}^{vis(i)}| = \frac{1}{2m_{\tilde{q}}} \left[\left((m_{\tilde{q}} + m_q)^2 - m_{\tilde{\chi}_1^0}^2 \right) \left((m_{\tilde{q}} - m_q)^2 - m_{\tilde{\chi}_1^0}^2 \right) \right]^{1/2}. \tag{55}$$

It is then straightforward to find that m_{T2} has a maximum at $\theta = 0$ for visible momenta in transverse direction, giving

$$
\begin{aligned}
m_{T2}^{\max} &= \frac{m_{\tilde{q}}^2 - m_{\tilde{\chi}_1^0}^2 + m_q^2}{2m_{\tilde{q}}} \\
&\quad + \sqrt{\frac{\left((m_{\tilde{q}} + m_q)^2 - m_{\tilde{\chi}_1^0}^2 \right) \left((m_{\tilde{q}} - m_q)^2 - m_{\tilde{\chi}_1^0}^2 \right)}{4m_{\tilde{q}}^2} + m_\chi^2}
\end{aligned} \tag{56}
$$

as obtained in (42). In the limit when the quark mass is negligible, this expression of $m_{T2}^{\max}$ is further simplified as

$$m_{T2}^{\max}(m_\chi) = \frac{m_{\tilde{q}}^2 - m_{\tilde{\chi}_1^0}^2}{2m_{\tilde{q}}} + \sqrt{\left(\frac{m_{\tilde{q}}^2 - m_{\tilde{\chi}_1^0}^2}{2m_{\tilde{q}}} \right)^2 + m_\chi^2}. \tag{57}$$

As the above $m_{T2}^{\max}$ has been obtained from a momentum configuration in which the two quarks produced by a squark pair at rest are moving in the same direction, one might worry that such two quarks might not be identified as two separate jets in real collider data with realistic jet reconstruction. However, the quark momenta from the back-to-back transverse boosted squark pair are generically not in the same direction, and thus the boosted events can provide two separate jets, while giving the same value of $m_{T2}^{\max}$.

To see explicitly some features of the squark m_{T2}, we have performed a Monte Carlo analysis for a SUSY parameter point in mirage mediation scenario [16], which gives

$$m_{\tilde{q}} = 697 \text{ GeV}, \quad m_{\tilde{\chi}_1^0} = 344 \text{ GeV}. \tag{58}$$

14

A Monte Carlo event sample for the signal $pp \rightarrow \tilde{q}\tilde{q} \rightarrow q\tilde{\chi}_1^0 q\tilde{\chi}_1^0$ has been generated in partonic-level using the PYTHIA event generator [17]. The m_{T2} values for the event sample were then calculated with a numerical code [18] implementing the minimization over the trial LSP momenta. Fig. 5(a) shows the resulting m_{T2} distribution for a trial LSP mass $m_\chi = 10$ GeV. The distribution shows a sharp edge at $m_{T2} = 527.8$ GeV, which is very close to $m_{T2}^{\max} = 527.4$ GeV obtained from the analytic formula (57). Finally, $m_{T2}^{\max}$ as a function of the trial LSP mass m_χ is shown in Fig. 5(b). Here, the blue curve represents the analytic formula (57), while the black dots are obtained from the Monte Carlo data, which fit very well the analytic curve.
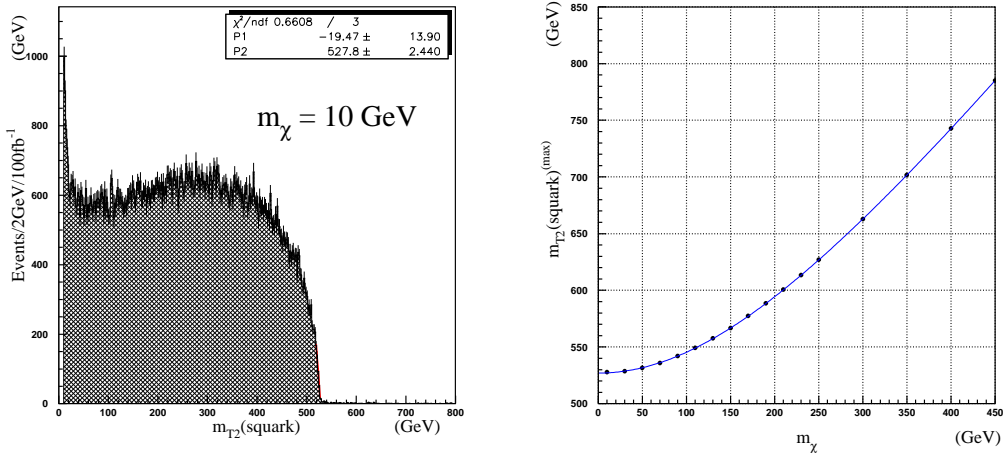

Figure 5: (a) m_{T2} distribution with $m_\chi = 10$ GeV for the mirage mediation parameter point (58). (b) Resulting $m_{T2}^{\max}$ as a function of the trial LSP mass m_χ.

Fig. 6 shows the distribution of the opening angle θ between the two visible quark momenta for the events near (a) the lower edge and (b) the upper edge of Fig. 5(a). As anticipated, the events near the lower edge and the upper edge give a distribution with a peak at $\cos\theta = -1$ and $\cos\theta = 1$, respectively. The rather broad peak in Fig. 6(b) is due to the non-zero transverse momentum of the each squark, which makes the two quarks from the squark-pair decay less aligned in general.

3.2 Gluino m_{T2}

Let us now examine a more complicate process in which each of the pair-produced mother particles decays into one invisible LSP and *more than one* visible particles, for which $m_{T2}^{\max}(m_\chi)$ shows a kink structure at $m_\chi = m_{\tilde{\chi}_1^0}$ as was noticed first in [6] and discussed in the previous section in a generic context. As a specific example, we consider the process
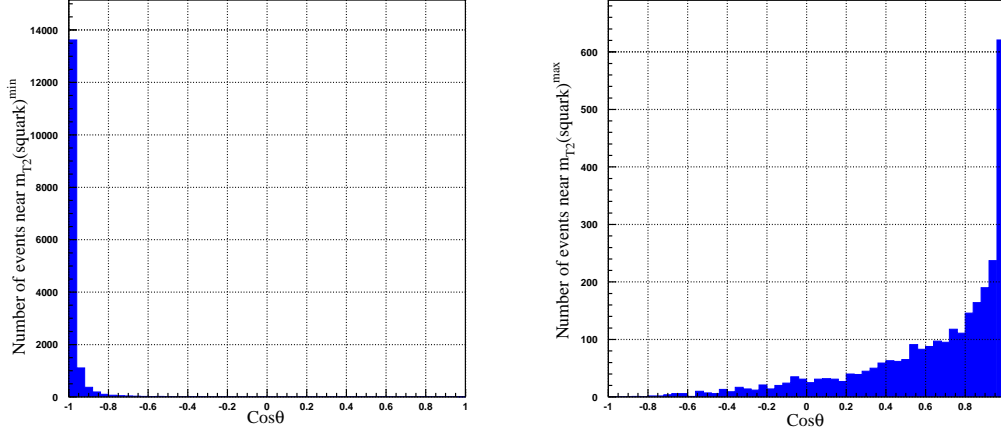
15

Figure 6: Event distribution along $\cos\theta$ for the events near (a) the lower edge and (b) the upper edge region of the Fig. 5(a).

in which a pair of gluinos are produced in proton-proton collision and each gluino decays into two quarks and one LSP:

$$pp \rightarrow \tilde{g}\tilde{g} \rightarrow qq\tilde{\chi}_1^0 qq\tilde{\chi}_1^0, \tag{59}$$

where again q denotes the 1st or 2nd generation quark. Depending upon whether squarks are heavier or lighter than gluino, the gluino decay $\tilde{g} \rightarrow qq\tilde{\chi}_1^0$ occurs through a three-body decay induced by an exchange of off-shell squark or two body cascade decay with intermediate on-shell squark. As noticed in the previous section, these two cases have a different value of $m_{vis}^{\max} = m_{qq}^{\max}$, thereby the resulting $m_{T2}^{\max}(m_\chi)$ has a different functional form in the range $m_\chi > m_{\tilde{\chi}_1^0}$.

For the process (59), the unconstrained minima of the transverse masses of the decay product of each gluino, i.e. $\left(m_T^{(i)}\right)_{\min} = m_{vis}^{(i)} + m_\chi$, are generically different from each other, thereby both of the balanced and unbalanced m_{T2} solutions can appear.

If the squark mass $m_{\tilde{q}}$ is heavier than the gluino mass $m_{\tilde{g}}$, gluino will undergo the three body decay $\tilde{g} \rightarrow qq\tilde{\chi}_1^0$ through an exchange of off-shell squark. In this case, for $m_q = 0$, the total invariant mass[¶] of the visible part of each gluino decay is in the following range:

$$0 \leq m_{vis}^{(1)}, m_{vis}^{(2)} \leq m_{\tilde{g}} - m_{\tilde{\chi}_1^0}. \tag{60}$$

As discussed in section 2, in order to obtain the maximum of gluino m_{T2}, we can limit ourselves to the situation that the two gluinos are produced at rest and all decay products

---

[¶]One might consider the total transverse mass of the visible part which has the same range.

16

are moving on the transverse plane. In such case, the transverse momentum and energy of the visible part are given by

$$
|\mathbf{p}_T^{vis(i)}| = \frac{\sqrt{\left((m_{\tilde{g}} + m_{vis}^{(i)})^2 - m_{\tilde{\chi}_1^0}^2\right)\left((m_{\tilde{g}} - m_{vis}^{(i)})^2 - m_{\tilde{\chi}_1^0}^2\right)}}{2m_{\tilde{g}}} \quad (i = 1, 2),
$$

$$
E_T^{vis(i)} = \frac{m_{\tilde{g}}^2 - m_{\tilde{\chi}_1^0}^2 + (m_{vis}^{(i)})^2}{2m_{\tilde{g}}}. \tag{61}
$$

Then, the balanced m_{T2} solution (25) is unambiguously fixed by the four variables: $m_{vis}^{(1)}$, $m_{vis}^{(2)}$, $\theta =$ the angle between $\mathbf{p}_T^{vis(1)}$ and $\mathbf{p}_T^{vis(2)}$, and the trial LSP mass m_χ.

For given values of $m_{vis}^{(i)}$ and m_χ, the maximum of the balanced m_{T2} occurs at $\theta = 0$ (see the appendix B for a detailed proof.) Since we are mainly interested in $m_{T2}^{\max}$, we will focus on the configuration with $\theta = 0$ in the following. From (25), we obtain

$$
m_{T2}^2|_{\theta=0} = m_\chi^2 + \tilde{A}
$$

$$
+ \sqrt{\left(1 + \frac{4m_\chi^2}{2\tilde{A} - \left(m_{vis}^{(1)}\right)^2 - \left(m_{vis}^{(2)}\right)^2}\right)\left(\tilde{A}^2 - \left(m_{vis}^{(1)} m_{vis}^{(2)}\right)^2\right)}, \tag{62}
$$

where

$$
\tilde{A} \equiv A|_{\theta=0} = E_T^{vis(1)} E_T^{vis(2)} + |\mathbf{p}_T^{vis(1)}||\mathbf{p}_T^{vis(2)}|, \tag{63}
$$

with $|\mathbf{p}_T^{vis(i)}|$ and $E_T^{vis(i)}$ given by (61). If we further restrict the momentum configurations to satisfy

$$
m_{vis}^{(1)} = m_{vis}^{(2)} \equiv m_{vis}, \tag{64}
$$

the balanced m_{T2} solution is simplified as

$$
m_{T2}|_{\theta=0} = \frac{m_{\tilde{g}}^2 - m_{\tilde{\chi}_1^0}^2 + m_{vis}^2}{2m_{\tilde{g}}}
$$

$$
+ \sqrt{\frac{\left((m_{\tilde{g}} + m_{vis})^2 - m_{\tilde{\chi}_1^0}^2\right)\left((m_{\tilde{g}} - m_{vis})^2 - m_{\tilde{\chi}_1^0}^2\right)}{4m_{\tilde{g}}^2} + m_\chi^2}. \tag{65}
$$

Then, from (41), we obtain

$$
m_{T2}^{\max}(m_\chi) = \frac{m_{\tilde{g}}^2 - m_{\tilde{\chi}_1^0}^2}{2m_{\tilde{g}}} + \sqrt{\left(\frac{m_{\tilde{g}}^2 - m_{\tilde{\chi}_1^0}^2}{2m_{\tilde{g}}}\right)^2 + m_\chi^2} \quad \text{if} \ \ m_\chi < m_{\tilde{\chi}_1^0}, \tag{66}
$$

$$
m_{T2}^{\max}(m_\chi) = \left(m_{\tilde{g}} - m_{\tilde{\chi}_1^0}\right) + m_\chi, \qquad\qquad \text{if} \ \ m_\chi > m_{\tilde{\chi}_1^0}. \tag{67}
$$

17

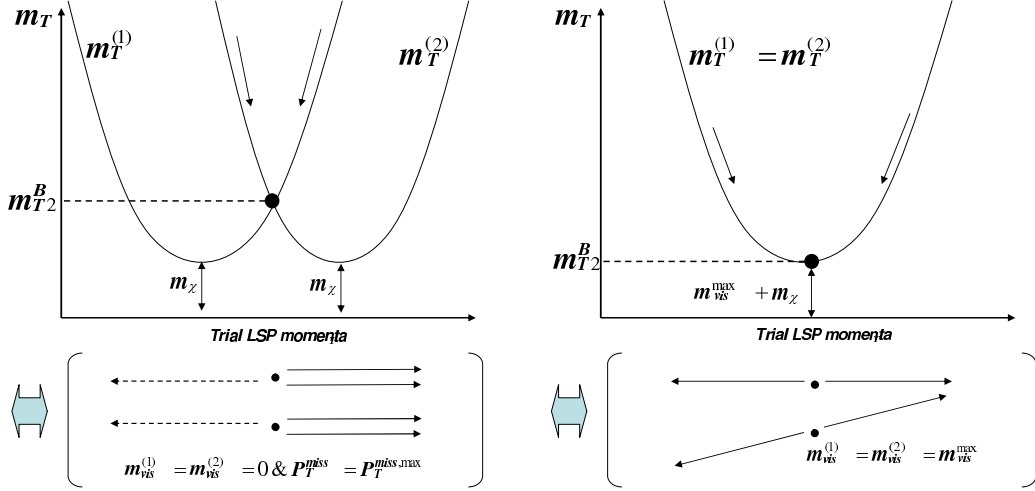Figure 7: Extreme momentum configuration providing $m_{T2}^{\max}$ as a balanced solution for (a) $m_\chi < m_{\tilde{\chi}_1^0}$ and (b) $m_\chi > m_{\tilde{\chi}_1^0}$.

Fig. 7(a) shows a momentum configuration providing the $m_{T2}^{\max}$ of (66). In this configuration, two gluinos are produced at rest, and each gluino subsequently decays into two quarks moving in the same direction (i.e. $m_{vis}^{(1)} = m_{vis}^{(2)} = 0$) and one LSP moving in the opposite direction. Furthermore, two sets of gluino decay products are parallel to each other (i.e. $\theta = 0$) and all of them are on the transverse plane with respect to the proton beam direction. This configuration is the first example of extreme momentum configuration considered in Ref. [6]. Although this corresponds to the simplest configuration providing the $m_{T2}^{\max}$ of (66), it might not be useful for constructing $m_{T2}^{\max}$ from real collider data as all quarks are moving in the same direction, so that they can not be identified as separate particles due to the finite jet resolution.

This difficulty of jet resolution can be partly avoided by the back-to-back transverse boost of the above extreme configuration, giving the same value of $m_{T2}^{\max}(m_\chi)$. In the back-to-back boosted configurations, the two di-quark systems are *not* moving in the same direction in general, so that can be distinguished from each other in real collider event. However, the two quarks in each di-quark system are still aligned to each other. In real collider data analysis, two aligned quarks cannot be identified as separate jets with realistic jet reconstruction, which will eliminate the events which involve the quarks moving in the same direction. As the true maximum of m_{T2} comes from such momentum configuration, any realistic jet reconstruction will cause a systematic shift of $m_{T2}^{\max}$ to a lower value when one tries to construct $m_{T2}^{\max}$ from real collider data. Our analytic expression (25) for the balanced m_{T2} solution provides information on how sensitive m_{T2} is to the angular separation of the involved quarks, with which one can estimate the

18

uncertainty of $m_{T2}^{\max}$ caused by the jet resolution cut:

$$\frac{\Delta m_{T2}^{\max}}{m_{T2}^{\max}} \approx -\frac{1}{8} \frac{m_{\tilde{\chi}_1^0}^2}{m_{\tilde{g}}^2} \left(1 - \frac{m_{\tilde{\chi}_1^0}^2}{m_{\tilde{g}}^2}\right) (\Delta R)^2 \lesssim \mathcal{O}(1)\,\%, \tag{68}$$

where $\Delta R \equiv \sqrt{\Delta\phi^2 + \Delta\eta^2} \sim 0.5$ represents a separation of two quarks in azimuthal angle and pseudorapidity plane. This indicates that the systematic shift of $m_{T2}^{\max}$ due to the finite jet resolution is negligible, which we have confirmed by an explicit Monte Carlo analysis.

The momentum configuration of Fig. 7(b) provides the $m_{T2}^{\max}$ of (67), which was considered in [6] as the second example of extreme momentum configuration. Here, gluinos are pair produced at rest, the two quarks from each gluino are back to back to each other ($m_{vis}^{(1)} = m_{vis}^{(2)} = m_{\tilde{g}} - m_{\tilde{\chi}_1^0}$), while the LSP is at rest. In this case, the angle θ is not well defined because $\mathbf{p}_T^{vis(1)} = \mathbf{p}_T^{vis(1)} = 0$. Also $\mathbf{p}_T^{miss} = 0$ which is true even after a back-to-back boost of the system. Such momentum configuration will be useless when one constructs $m_{T2}^{\max}$ from collider data as one typically uses an event selection cut imposing a lower bound on $|\mathbf{p}_T^{miss}|$. However, as we will see shortly, there exist momentum configurations yielding (67) while having a sizable $|\mathbf{p}_T^{miss}|$, so that the $m_{T2}^{\max}$ of (67) can be constructed from collider data even under a proper cut on $|\mathbf{p}_T^{miss}|$.
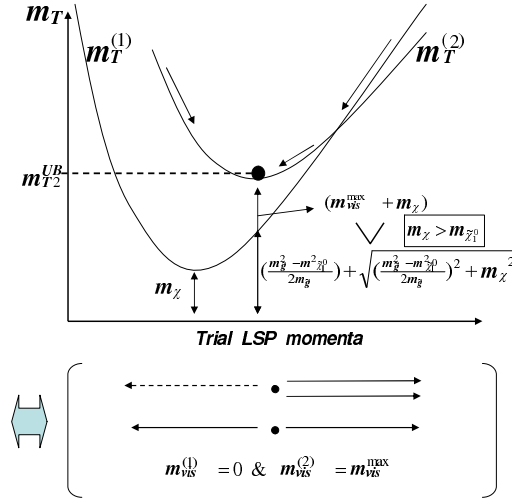

Figure 8: Extreme momentum configuration providing $m_{T2}^{\max}$ as an unbalanced solution for $m_\chi > m_{\tilde{\chi}_1^0}$.

A momentum configuration, which provides the $m_{T2}^{\max}$ of (67) with a sizable $|\mathbf{p}_T^{miss}|$, is shown in Fig.8. In this configuration, two gluinos are produced at rest. The first

19

gluino produces a di-quark system with $m_{vis}^{(1)} = 0$ and one LSP, while the second gluino produces a back-to-back di-quark system with $m_{vis}^{(2)} = m_{\tilde{g}} - m_{\tilde{\chi}_1^0}$ and one LSP at rest. For the second gluino decay set, the visible momentum $\mathbf{p}_T^{vis(2)} = 0$. Thus, unconstrained minimum of the second gluino transverse mass, $m_T^{(2)} = (m_{\tilde{g}} - m_{\tilde{\chi}_1^0}) + m_\chi$, occurs when trial LSP momentum $\mathbf{p}_T^{\chi(2)} = 0$. On the other hand, the first gluino decay product has $|\mathbf{p}_T^{vis(1)}| = (m_{\tilde{g}}^2 - m_{\tilde{\chi}_1^0}^2)/2m_{\tilde{g}}$ and $\mathbf{p}_T^{\chi(1)} = -\mathbf{p}_T^{vis(1)}$, for $\mathbf{p}_T^{\chi(2)} = 0$. Then, the corresponding transverse mass of the first gluino decay is given by

$$m_T^{(1)} = \frac{m_{\tilde{g}}^2 - m_{\tilde{\chi}_1^0}^2}{2m_{\tilde{g}}} + \sqrt{\left(\frac{m_{\tilde{g}}^2 - m_{\tilde{\chi}_1^0}^2}{2m_{\tilde{g}}}\right)^2 + m_\chi^2}. \tag{69}$$

Therefore, $m_T^{(2)} > m_T^{(1)}$ if $m_\chi > m_{\tilde{\chi}_1^0}$, though $m_T^{(2)}$ is at the unconstrained minimum value, so that we have unbalanced m_{T2} solution, i.e. $m_{T2} = (m_{\tilde{g}} - m_{\tilde{\chi}_1^0}) + m_\chi$ for this momentum configuration. The same unbalanced m_{T2} solution is obtained for the momentum configuration with other values of $m_{vis}^{(1)}$ because those cases also give $m_T^{(2)} \geq m_T^{(1)}$ when $m_T^{(2)}$ is at the unconstrained minimum. Such momentum configurations and the back-to-back transverse boosted ones would have a sizable $|\mathbf{p}_T^{miss}|$, so can be used to determine m_{T2}^{max} from real collider data.

To summarize the extremal features of m_{T2} for the decay of gluino pair when $m_{\tilde{q}} > m_{\tilde{g}}$, the maximum of m_{T2} over all events is given by

$$\begin{aligned}
m_{T2}^{max}(m_\chi) &= \frac{m_{\tilde{g}}^2 - m_{\tilde{\chi}_1^0}^2}{2m_{\tilde{g}}} + \sqrt{\left(\frac{m_{\tilde{g}}^2 - m_{\tilde{\chi}_1^0}^2}{2m_{\tilde{g}}}\right)^2 + m_\chi^2} \quad \text{if} \quad m_\chi < m_{\tilde{\chi}_1^0}, \\
m_{T2}^{max}(m_\chi) &= \left(m_{\tilde{g}} - m_{\tilde{\chi}_1^0}\right) + m_\chi \quad \text{if} \quad m_\chi > m_{\tilde{\chi}_1^0}
\end{aligned} \tag{70}$$

as obtained in (45) and (47) in more generic context. Thus, there is a level crossing of m_{T2}^{max} at $m_\chi = m_{\tilde{\chi}_1^0}$, yielding a kink structure as shown in Fig. 4(a). If such m_{T2}^{max}-curve can be constructed from collider data, which will be examined in the next subsection, this kink structure will enable us to determine the true LSP mass $m_{\tilde{\chi}_1^0}$ and the gluino mass $m_{\tilde{g}} = m_{T2}^{max}(m_\chi = m_{\tilde{\chi}_1^0})$ *simultaneously*.

To see explicitly the extremal features of gluino m_{T2}, a Monte Carlo event sample of the signal $pp \to \tilde{g}\tilde{g} \to qq\tilde{\chi}_1^0 qq\tilde{\chi}_1^0$ has been generated in partonic-level, for a SUSY parameter point in a minimal anomaly mediated SUSY-breaking (AMSB) scenario [19], which gives

$$m_{\tilde{g}} = 780 \text{ GeV}, \quad m_{\tilde{\chi}_1^0} = 98 \text{ GeV}, \tag{71}$$

with a few TeV sfermion masses. The m_{T2} values for the event sample were then calculated. Fig.9 (a) and (b) show the resulting m_{T2} distributions for trial LSP mass $m_\chi = 10$
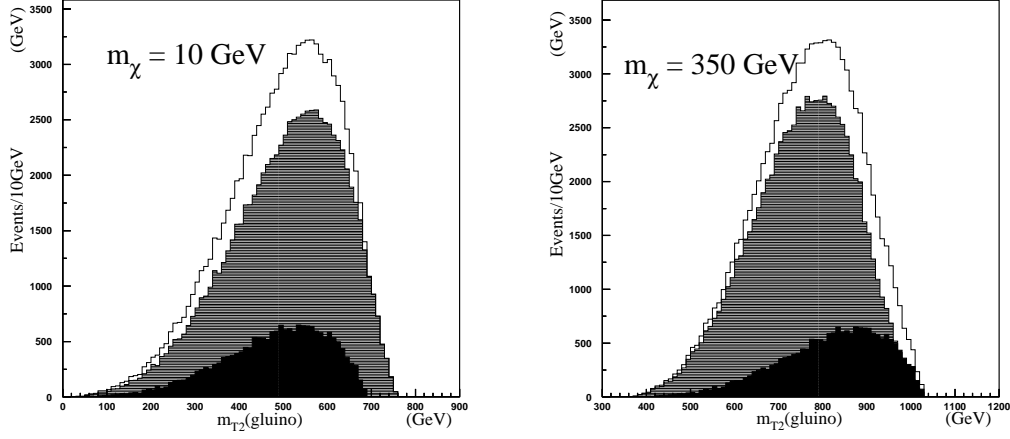
Figure 9: m_{T2} distribution with (a) $m_\chi = 10$ GeV and (b) $m_\chi = 350$ GeV for the AMSB parameter point (71).
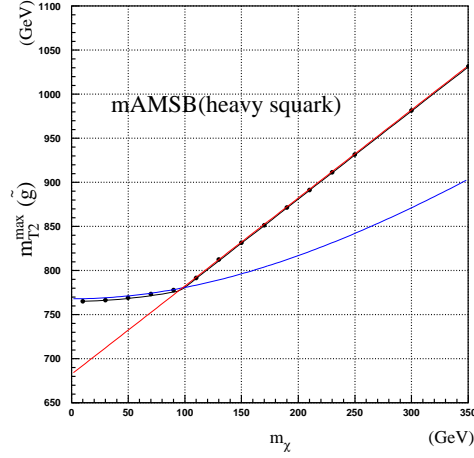

Figure 10: $m_{T2}^{\max}$ as a function of the trial LSP mass m_χ for the AMSB parameter point (71).

GeV and 350 GeV, respectively. On the figures, hatched histogram corresponds to the balanced m_{T2} values, while black histogram to the unbalanced ones. As anticipated, one can notice that for $m_\chi = 10$ GeV, which is smaller than true LSP mass, the endpoint of the m_{T2} distribution is determined by the balanced m_{T2} solutions, while both balanced

21

and unbalanced m_{T2} solution contribute to the endpoint region for $m_\chi = 350$ GeV, which is larger than true LSP mass. Finally, $m_{T2}^{\max}$ as a function of the trial LSP mass m_χ is shown in Fig. 10. Here, the blue and red curves represent the analytic formula (70), while the black dots are obtained from the Monte Carlo data, which fit very well the analytic curves.

Let us now consider the case of lighter squark, $m_{\tilde{q}} < m_{\tilde{g}}$, for which the following cascade decay is open:

$$\tilde{g} \to q\tilde{q} \to qq\tilde{\chi}_1^0, \tag{72}$$

where the squark in the second stage is on mass-shell. The main difference between this two body cascade decay and the three body decay is that the total invariant mass of the visible part takes the range:

$$0 \leq m_{vis}^{(1)}, \, m_{vis}^{(2)} \leq \sqrt{\frac{(m_{\tilde{g}}^2 - m_{\tilde{q}}^2)(m_{\tilde{q}}^2 - m_{\tilde{\chi}_1^0}^2)}{m_{\tilde{q}}^2}}. \tag{73}$$

As $m_{vis}^{\max}$ has a smaller value than the three body decay case, while $m_{vis}^{\min}$ is same, the kink structure is weakened as was anticipated in (44). The maximum of m_{T2} for $m_\chi < m_{\tilde{\chi}_1^0}$ takes the same form as the case of heavier squarks, while it is changed to a different form for $m_\chi > m_{\tilde{\chi}_1^0}$:

$$m_{T2}^{\max}(m_\chi) = \frac{m_{\tilde{g}}^2 - m_{\tilde{\chi}_1^0}^2}{2m_{\tilde{g}}} + \sqrt{\left(\frac{m_{\tilde{g}}^2 - m_{\tilde{\chi}_1^0}^2}{2m_{\tilde{g}}}\right)^2 + m_\chi^2} \quad \text{if} \quad m_\chi < m_{\tilde{\chi}_1^0},$$

$$m_{T2}^{\max}(m_\chi) = \left(\frac{m_{\tilde{g}}}{2}(1 - \frac{m_{\tilde{q}}^2}{m_{\tilde{g}}^2}) + \frac{m_{\tilde{g}}}{2}(1 - \frac{m_{\tilde{\chi}_1^0}^2}{m_{\tilde{q}}^2})\right)$$

$$+ \sqrt{\left(\frac{m_{\tilde{g}}}{2}(1 - \frac{m_{\tilde{q}}^2}{m_{\tilde{g}}^2}) - \frac{m_{\tilde{g}}}{2}(1 - \frac{m_{\tilde{\chi}_1^0}^2}{m_{\tilde{q}}^2})\right)^2 + m_\chi^2} \quad \text{if} \quad m_\chi > m_{\tilde{\chi}_1^0} \tag{74}$$

as obtained in (49). The $m_{T2}^{\max}$-curve for lighter squarks is depicted in Fig. 4(b), which shows again a kink structure at $m_\chi = m_{\tilde{\chi}_1^0}$, although milder than the case of heavier squarks. Note that the $m_{T2}^{\max}$-curve for the range $m_\chi > m_{\tilde{\chi}_1^0}$ depends on the squark mass also, so it can determine the gluino mass, the LSP mass and the squark mass altogether.

3.3 Construction of gluino m_{T2} from collider data

In order to check the experimental feasibility of measuring superparticle masses using the kink structure of the gluino $m_{T2}^{\max}$, we have generated Monte Carlo event samples of the SUSY signals at LHC by PYTHIA [17] for several SUSY breaking schemes yielding

different patterns of superparticle spectra. We have also generated the SM backgrounds such as $t\bar{t}$, W/Z + jet, $WW/WZ/ZZ$ and QCD events, with less equivalent luminosity, in five logarithmic p_T bins for 50 GeV $< p_T <$ 4000 GeV. The SM backgrounds have been also generated by PYTHIA. The generated events have been further processed with a modified version of the fast detector simulation program PGS [20], which approximates an ATLAS or CMS-like detector with reasonable efficiencies and fake rates.

For each event, the four leading jets are used to calculate the gluino m_{T2}. For a convenience of numerical analysis, we considered m_{T2} defined in terms of the transverse visible mass $m_T^{vis(i)}$, rather than in terms of the invariant visible mass $m_{vis}^{(i)}$, which gives the same value of $m_{T2}^{\max}$ as remarked in section 2. Note that $m_T^{vis(i)} = m_{vis}^{(i)}$ for the extreme momentum configurations giving the maximal value of m_{T2}. The four jets are divided in two groups of dijets as follows [21]. The highest momentum jet and the other jet which has the largest $|p_{jet}|\Delta R$ with respect to the leading jet are chosen as two 'seed' jets for the division. Here, p_{jet} is the jet momentum and $\Delta R \equiv \sqrt{\Delta\phi^2 + \Delta\eta^2}$ denotes the jet separation in azimuthal angle and pseudorapidity plane. Each of the remaining two jets is associated to the seed jet making a smaller opening angle. Then, each of the jet pairs constructed in this way is considered to be originating from the same mother particle (gluino). If this procedure fails to choose two groups of jet pairs, we discarded the event.

Because the functional form of the gluino $m_{T2}^{\max}(m_\chi)$ depends upon whether the 1st and 2nd generations of squarks are heavier than gluino or not, we consider those two cases separately. Let us first consider the case of heavier squarks. Superparticle spectrum with $m_{\tilde{q}} > m_{\tilde{g}}$ can arise from various SUSY breaking schemes, for which the gluino m_{T2} takes the form of Fig. 4(a). For simplicity, here we consider only the case that the 1st and 2nd generations of squarks are significantly heavier than 1 TeV, e.g. $m_{\tilde{q}} \sim 4$ TeV, so that squarks are *not* copiously produced at LHC[||], while gluino is light enough to be copiously produced, e.g. $m_{\tilde{g}} < 1$ TeV. As an specific example of such superparticle spectrum, here we consider a parameter point of anomaly mediation scenario (AMSB) with heavy sfermion masses, in which the gluino, LSP and (the 1st and 2nd generation) squark masses are given by[**]

$$\text{AMSB with heavy sfermions}: m_{\tilde{g}} = 780\,\text{GeV}, \quad m_{\tilde{\chi}_1^0} = 98\,\text{GeV}, \quad m_{\tilde{q}} = 4\,\text{TeV}. \quad (75)$$

For the AMSB point, the production cross section of gluino pair $\sigma(\tilde{g}\tilde{g}) \sim 1.1$pb. The branching ratios of gluino decay are as follows: $B(\tilde{g} \to \tilde{\chi}_1^0 qq) \sim 32\%$, $B(\tilde{g} \to \tilde{\chi}_2^0 qq) \sim 3\%$, $B(\tilde{g} \to \tilde{\chi}_1^\pm qq') \sim 64\%$. Thus, gluino mostly decays into lighter chargino (or LSP) plus two

---

[||]If squarks are heavier than gluino, but still light enough to be copiously produced at LHC, the gluino m_{T2} is not a proper observable to determine the gluino and LSP masses since the gluino-pair events $\tilde{g}\tilde{g} \to qq\tilde{\chi}_1^0 qq\tilde{\chi}_1^0$ are severely screened by the squark pair events $\tilde{q}\tilde{q} \to q\tilde{g}q\tilde{g} \to qqq\tilde{\chi}_1^0 qqq\tilde{\chi}_1^0$. In such case, one can construct the squark m_{T2} for the squark pair events with six quarks, which would show a behavior similar to the gluino $m_{T2}^{\max}$ in the case of lighter squark, from which the squark, gluino, and LSP masses can be determined altogether.

[**]We also assume $\tan\beta = 10$ and the Higgsino mass parameter $\mu > 0$.

quarks. Being wino-like, the LSP and the lighter chargino are almost degenerate in mass. The chargino decay $\tilde{\chi}_1^\pm \to \tilde{\chi}_1^0 l^\pm \nu$ produces very soft leptons, which cannot be detected at LHC. In this circumstance, both gluino decays $\tilde{g} \to \tilde{\chi}_1^\pm qq'$ and $\tilde{g} \to \tilde{\chi}_1^0 qq$ can be considered as 'signals' we are looking for, and the contamination from the small number of $\tilde{g} \to \tilde{\chi}_2^0 qq$ decay is expected not to be significant. In this work, we assume integrated luminosity of $300 \; fb^{-1}$ for the AMSB point.
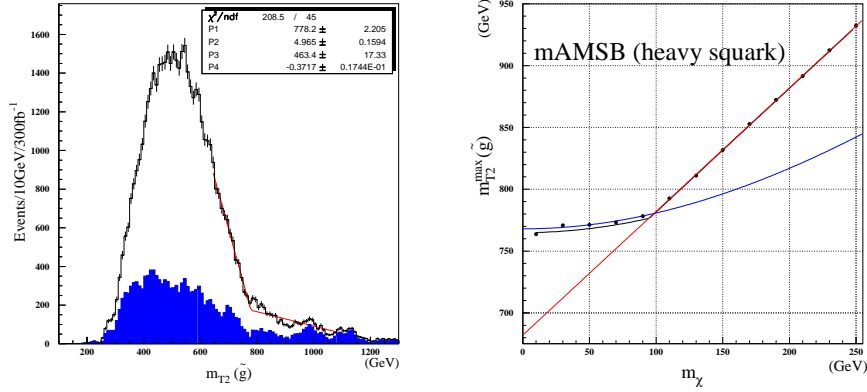

Figure 11: (a) Gluino m_{T2} distribution with $m_\chi = 90$ GeV for AMSB with heavy sfermions, and (b) $m_{T2}^{\max}$ as a function of m_χ for AMSB with heavy sfermions.

To obtain a clean signal sample for the gluino m_{T2}, we have imposed the following event selection cuts on the SUSY and SM event samples.

1. At least 4 jets with $P_{T1,2,3,4} > 200, 150, 100, 50$ GeV.

2. Missing transverse energy $E_T^{miss} > 250$ GeV.

3. Transverse sphericity $S_T > 0.25$.

4. No b-jets and no leptons.

Using the event set passing these selection cuts, we calculate the gluino m_{T2} for various values of the trial LSP mass m_χ. Fig. 11 (a) shows the resulting gluino m_{T2} distributions for the AMSB with $m_\chi = 90$ GeV. Fitting the distribution with a linear function with a linear background, we get the endpoint value

$$\text{AMSB}: m_{T2}^{\max}(m_\chi = 90) = 778.2 \pm 2.2 \text{ GeV} \tag{76}$$

The edge values of m_{T2} obtained in this way are shown in Fig. 11 (b). Blue and red lines denote the theoretical curves obtained from (70). Fitting the data points to these curves,

24

we obtain the following gluino and LSP masses:

$$\text{AMSB}: \; m_{\tilde{g}} = 776.5 \pm 1.0, \quad m_{\tilde{\chi}_1^0} = 94.9 \pm 1.4 \text{ GeV}, \tag{77}$$

which are quite close to the true values in (75). This demonstrates that the gluino m_{T2} can be very useful for measuring the gluino and the LSP masses experimentally in heavier squark scenario.

Let us now consider the case of lighter squarks, $m_{\tilde{q}} < m_{\tilde{g}}$, for which the cascade decay $\tilde{g} \to q\tilde{q} \to qq\chi_1^0$ is open. As an example of superparticle spectra with lighter squarks, we choose a parameter point (SPS1a [22]) of mSUGRA schemes, which provides

$$\text{mSUGRA with light squarks}: \; m_{\tilde{g}} = 613, \quad m_{\tilde{q}} = 525, \quad m_{\tilde{\chi}_1^0} = 99 \text{ GeV}. \tag{78}$$

For this mSUGRA point, the production cross sections for $\tilde{g}\tilde{g}$, $\tilde{g}\tilde{q}$ and $\tilde{q}\tilde{q}$ pairs are $\sigma(\tilde{g}\tilde{g}) \sim 4.2$ pb, $\sigma(\tilde{g}\tilde{q}) \sim 21$ pb, and $\sigma(\tilde{q}\tilde{q}) \sim 9$ pb, respectively. The branching ratio of the signal decay chain, i.e, $\tilde{g} \to \tilde{q}q \to \tilde{\chi}_1^0 qq$ is $B(\tilde{g} \to \tilde{\chi}_1^0 qq) \sim 40\%$, while corresponding branching ratios to $\tilde{\chi}_2^0$, and $\tilde{\chi}_1^\pm$ are $B(\tilde{g} \to \tilde{\chi}_2^0 qq) \sim 7\%$, and $B(\tilde{g} \to \tilde{\chi}_1^\pm qq') \sim 14\%$, respectively. Here, we assume 30 fb^{-1} of integrated luminosity for the mSUGRA point.

Similarly to the above AMSB case, we have imposed following event selection cuts:

1. Missing transverse energy $E_T^{miss} > 250$ GeV.

2. Transverse sphericity $S_T > 0.25$.

3. No b-jets and no leptons.

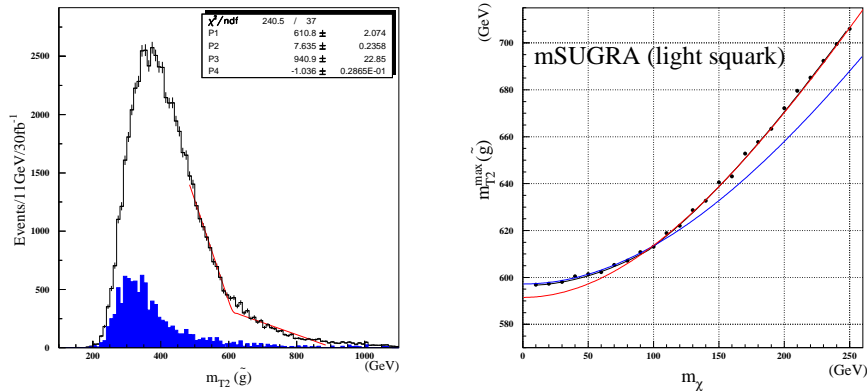

Figure 12: Gluino m_{T2} distribution with (a) $m_\chi = 90$ GeV for the mSUGRA point with light squarks, and (b) m_{T2}^{max} as a function of m_χ for mSUGRA with light squarks.

25

Again using the Monte Carlo events passing the selection cuts, we evaluated gluino m_{T2}. Fig.12 (a) shows the m_{T2} distribution for trial LSP mass $m_\chi = 90$ in mSUGRA scenario with light squark. Even with the above selection cuts, the events from the $\tilde{g}\tilde{q}$ pair production largely contribute to the m_{T2} distribution. The contribution from $\tilde{g}\tilde{q}$ pair events provides rather similar shape of m_{T2} distribution to the one from $\tilde{g}\tilde{g}$ events, but the maximum of m_{T2} from $\tilde{g}\tilde{q}$ events is still smaller than the one from $\tilde{g}\tilde{g}$ events.

Fitting the edges of these distributions, we find the endpoint values:

$$\text{mSUGRA} : m_{T2}^{\max}(m_\chi = 90) = 610.8 \pm 2.1 \text{ GeV}. \tag{79}$$

Fig.12 (b) shows $m_{T2}^{\max}$ as a function of m_χ. Fitting the data points to the analytic expression (74), we obtain

$$\text{mSUGRA} : m_{\tilde{g}} = 611.7 \pm 2.8, \quad m_{\tilde{q}} = 519.9 \pm 2.8, \quad m_{\tilde{\chi}_1^0} = 96.3 \pm 8.1 \text{ GeV}. \tag{80}$$

which are again quite close to the true mass values in (78). We have performed the same analysis for other superparticle spectra with $m_{\tilde{q}} < m_{\tilde{g}}$, e.g. a parameter point of mirage mediation scenario [16], and found that the gluino mass, squark mass and LSP mass can be determined with a similar accuracy.

Here, we emphasize that the above results include only the statistical uncertainties. There should be various systematic uncertainties associated with the choice of fit function and the fit range to determine the endpoint of m_{T2} distribution, which would affect the result. Study of such systematic uncertainties, however, is beyond the scope of this work.

4 Conclusion

In this paper, we provided a detailed study of the collider observable m_{T2} applied for pair-produced superparticles decaying to visible particles and a pair of invisible LSPs. In particular, we have derived the analytic expression of the maximum of m_{T2} over all events $(m_{T2}^{\max})$. It is noticed that if the decay product of each superparticle involves more than one visible particle, $m_{T2}^{\max}$ being a function of the *trial* LSP mass m_χ has a kink structure, i.e. a continuous but not differentiable cusp, at $m_\chi = $ true LSP mass, which can be used to determine the mother superparticle mass and the LSP mass simultaneously. The sharpness of the kink structure depends on whether the full decay process involves an intermediate on-shell particle (lighter than the mother particle) or not. In case without any intermediate on-shell particle, the kink structure is sharper. In other case with an intermediate on-shell particle, although the kink structure is weakened, the $m_{T2}^{\max}$-curve can be used to determine the intermediate particle mass also.

We also performed a Monte-Carlo study of the gluino m_{T2} for some superparticle spectra in order to examine how well $m_{T2}^{\max}$ can be constructed from collider data. The result of our study indicates that the kink structure of $m_{T2}^{\max}$ can be quite useful for the determination of superparticle masses in many cases, and determine the mother particle mass and the LSP mass quite accurately in some cases.

Acknowledgements

Appendix A

In this appendix, we show that m_{T2} of any event in the laboratory frame is bounded above by another m_{T2} of an event induced by mother particle pair *at rest*. Let us consider generic event induced by a symmetric decay of mother particle pair:

$$\Phi_i \rightarrow \tilde{\chi}_1^0 + \text{visible particle(s)}, \tag{81}$$

and let $\mathbf{p}^{vis(i)}$ ($i = 1, 2$) denote the total visible momentum of the decay product of Φ_i measured in the laboratory frame. The corresponding m_{T2} is determined by the visible transverse momenta $\mathbf{p}_T^{vis(i)}$ and the visible invariant masses $m_{vis}^{(i)}$ as defined in (5):

$$m_{T2}(\mathbf{p}_T^{vis(i)}, m_{vis}^{(i)}, m_\chi) = \min_{\{\mathbf{p}_T^{\chi(1)}+\mathbf{p}_T^{\chi(2)}=-\mathbf{p}_T^{vis(1)}-\mathbf{p}_T^{vis(2)}\}} \left[\max\left\{ m_T^{(1)}, m_T^{(2)} \right\} \right], \tag{82}$$

where

$$m_T^{(i)} = \sqrt{m_\chi^2 + (m_{vis}^{(i)})^2 + 2E_T^{vis(i)} E_T^{\chi(i)} - 2\mathbf{p}_T^{vis(i)} \cdot \mathbf{p}_T^{\chi(i)}}. \tag{83}$$

As the first step, let us perform independent longitudinal boost of mother particles to make the mother particle pair to move back-to-back in transverse direction. Note that one can always make such longitudinal boost for mother particle pair having a vanishing total transverse momentum in the laboratory frame, and also the required longitudinal boost of Φ_1 is generically different from the one of Φ_2. Let $\mathbf{p}^{\prime vis(i)}$ denote the visible momentum after such longitudinal boost of mother particles. As $\mathbf{p}_T$ and $E_T = \sqrt{m^2 + |\mathbf{p}_T|^2}$ are invariant under longitudinal boost, we obviously have

$$m_{T2}(\mathbf{p}_T^{vis(i)}, m_{vis}^{(i)}, m_\chi) = m_{T2}(\mathbf{p}^{\prime vis(i)}, m_{vis}^{(i)}, m_\chi). \tag{84}$$

To proceed, let us consider the generalized invariant mass m_{I2} defined as follows:

$$m_{I2}(\mathbf{p}^{vis(i)}, m_{vis}^{(i)}, m_\chi) = \min_{\{\mathbf{p}^{\chi(1)}+\mathbf{p}^{\chi(2)}=-\mathbf{p}^{vis(1)}-\mathbf{p}^{vis(2)}\}} \left[\max\left\{ m^{(1)}, m^{(2)} \right\} \right], \tag{85}$$

where $m^{(i)}$ is the trial invariant mass of the mother particle Φ_i obtained for the trial LSP mass m_χ:

$$m^{(i)} = \sqrt{m_\chi^2 + (m_{vis}^{(i)})^2 + 2E^{vis(i)} E^{\chi(i)} - 2\mathbf{p}^{vis(i)} \cdot \mathbf{p}^{\chi(i)}}, \tag{86}$$

and the minimization is performed over the trial LSP momenta satisfying

$$\mathbf{p}^{\chi(1)} + \mathbf{p}^{\chi(2)} = -\mathbf{p}^{vis(1)} - \mathbf{p}^{vis(2)}. \tag{87}$$

As $m_T^{(i)} \leq m^{(i)}$ for arbitrary visible and trial momenta, one immediately finds

$$m_{T2}(\mathbf{p}_T^{\prime vis(i)}, m_{vis}^{(i)}, m_\chi) \leq m_{I2}(\mathbf{p}^{\prime vis(i)}, m_{vis}^{(i)}, m_\chi), \tag{88}$$

where the equality holds for $\mathbf{p}'^{vis(i)}$ in T-direction. Note that m_{I2} can be considered as an $(1+3)$-dimensional analogue of the $(1+2)$-dimensional m_{T2}.

The global minimum of $m^{(i)}$ over the unconstrained $\mathbf{p}^{\chi(i)}$ is given by

$$\left(m^{(i)}\right)_{\min} = m_{vis}^{(i)} + m_\chi, \tag{89}$$

which occurs when

$$\mathbf{p}^{\chi(i)} = E^{\chi(i)}\mathbf{p}^{vis(i)}/E^{vis(i)} = m_\chi \mathbf{p}^{vis(i)}/m_{vis}^{(i)}. \tag{90}$$

Like m_{T2}, the generalized invariant mass m_{I2} is also given by either a balanced solution or an unbalanced solution. If $m^{(i)} \geq m^{(j)}$ for both i when the trial LSP momenta take the value giving the unconstrained minimum of $m^{(j)}$ $(j \neq i)$, i.e. if

$$\left. m^{(1)}\right|_{\mathbf{p}^{\chi(1)}=-\mathbf{p}^{vis(1)}-\mathbf{p}^{vis(2)}-\tilde{\mathbf{p}}^{\chi(2)}} \geq \left. m^{(2)}\right|_{\mathbf{p}^{\chi(2)}=\tilde{\mathbf{p}}^{\chi(2)}} = m_{vis}^{(2)} + m_\chi,$$
$$\left. m^{(2)}\right|_{\mathbf{p}^{\chi(2)}=-\mathbf{p}^{vis(1)}-\mathbf{p}^{vis(2)}-\tilde{\mathbf{p}}^{\chi(1)}} \geq \left. m^{(1)}\right|_{\mathbf{p}^{\chi(1)}=\tilde{\mathbf{p}}^{\chi(1)}} = m_{vis}^{(1)} + m_\chi, \tag{91}$$

where

$$\tilde{\mathbf{p}}^{\chi(i)}/m_\chi = \mathbf{p}^{vis(i)}/m_{vis}^{(i)},$$

the corresponding m_{I2} is given by a balanced solution:

$$m_{I2} = m_{I2}^{\mathrm{bal}} = \min_{\{\mathbf{p}^{\chi(1)}+\mathbf{p}^{\chi(2)}=-\mathbf{p}^{vis(1)}-\mathbf{p}^{vis(2)}, m^{(1)}=m^{(2)}\}} \left[m^{(1)}\right], \tag{92}$$

where the minimization is performed over $\mathbf{p}^{\chi(i)}$ satisfying

$$m^{(1)}(\mathbf{p}^{vis(1)}, \mathbf{p}^{\chi(1)}, m_{vis}^{(1)}, m_\chi) = m^{(2)}(\mathbf{p}^{vis(2)}, \mathbf{p}^{\chi(2)}, m_{vis}^{(2)}, m_\chi),$$
$$\mathbf{p}^{\chi(1)} + \mathbf{p}^{\chi(2)} = -\mathbf{p}^{vis(1)} - \mathbf{p}^{vis(2)}. \tag{93}$$

On the other hand, if $m^{(i)} \leq m^{(j)}$ for any i when the trial LSP momenta take the value giving the unconstrained minimum of $m^{(j)}$ $(j \neq i)$, i.e. if

$$\left. m^{(i)}\right|_{\mathbf{p}^{\chi(i)}=\tilde{\mathbf{p}}^{\chi(i)}} \leq \left. m^{(j)}\right|_{\mathbf{p}^{\chi(j)}=\tilde{\mathbf{p}}^{\chi(j)}} \quad (j \neq i) \tag{94}$$

for the trial LSP momenta given by

$$\tilde{\mathbf{p}}^{\chi(j)} = \tilde{\mathbf{p}}^{\chi(1)} = m_\chi \mathbf{p}^{vis(1)}/m_{vis}^{(1)},$$
$$\tilde{\mathbf{p}}^{\chi(2)} = -\mathbf{p}^{vis(1)} - \mathbf{p}^{vis(2)} - \tilde{\mathbf{p}}^{\chi(1)}, \tag{95}$$

or

$$\tilde{\mathbf{p}}^{\chi(j)} = \tilde{\mathbf{p}}^{\chi(2)} = m_\chi \mathbf{p}^{vis(2)}/m_{vis}^{(2)},$$
$$\tilde{\mathbf{p}}^{\chi(1)} = -\mathbf{p}^{vis(1)} - \mathbf{p}^{vis(2)} - \tilde{\mathbf{p}}^{\chi(2)}, \tag{96}$$

29

the corresponding m_{I2} is given by an unbalanced solution as

$$m_{I2} = m_{I2}^{\text{unbal}} = m_{vis}^{(j)} + m_\chi \quad (j = 1 \text{ or } 2). \tag{97}$$

In section 2, we have noticed that m_{T2} is invariant under the back-to-back boost of $\mathbf{p}^{vis(i)}$ along the direction of the transverse plane T, if both $\mathbf{p}^{vis(1)}$ and $\mathbf{p}^{vis(2)}$ are in the direction of T. It is in fact straightforward to show that m_{I2} is invariant under back-to-back boost in general direction for general $\mathbf{p}^{vis(i)}$, which corresponds to the $(1+3)$-dimensional version of the back-to-back boost invariance of m_{T2}. To show this, let us first note that the invariant masses $m^{(i)}$ and the relations (91) and (93) are invariant or covariant under the following back-to-back Lorentz boost:

$$\begin{aligned} \alpha_1^\mu &\to \Lambda^\mu_\nu(\vec{v})\alpha_1^\nu, \quad \beta_1^\mu \to \Lambda^\mu_\nu(\vec{v})\beta_1^\nu, \\ \alpha_2^\mu &\to \Lambda^\mu_\nu(-\vec{v})\alpha_2^\nu, \quad \beta_2^\mu \to \Lambda^\mu_\nu(-\vec{v})\beta_2^\nu, \end{aligned} \tag{98}$$

where $\alpha_i^\mu = (E^{vis(i)}, \mathbf{p}^{vis(i)})$ are the visible 4-momenta, $\beta_i^\mu = (E^{\chi(i)}, \mathbf{p}^{\chi(i)})$ are the trial LSP 4-momenta, and $\Lambda^\mu_\nu(\vec{v})$ denotes the $(1+3)$-dimensional Lorentz transformation for generic 3-dimensional boost parameter $\vec{v}$. This assures that m_{I2} given by a balanced solution is invariant under generic back-to-back boost, which can be confirmed by the following explicit form of m_{I2}^{bal}:

$$\begin{aligned} \left(m_{I2}^{\text{bal}}\right)^2 &= m_\chi^2 + A \\ &+ \sqrt{\left(1 + \frac{4m_\chi^2}{2A - \left(m_{vis}^{(1)}\right)^2 - \left(m_{vis}^{(2)}\right)^2}\right)\left(A^2 - \left(m_{vis}^{(1)}m_{vis}^{(2)}\right)^2\right)}, \end{aligned} \tag{99}$$

where A is the Euclidean product of the two visible 4-momenta α_1^μ and α_2^μ:

$$A = E^{vis(1)}E^{vis(2)} + \mathbf{p}^{vis(1)} \cdot \mathbf{p}^{vis(2)}. \tag{100}$$

Similarly, the relations (94) and (95) are covariant under the above back-to-back Lorentz boost, so m_{I2} given by an unbalanced solution is invariant also.

In fact, the covariance of (91) and (94) under the back-to-back boost (98), which we have used to show the invariance of m_{I2}, is not so obvious. The easiest way to see their covariance is to consider the boundary between (91) and (94), which corresponds to the visible momenta satisfying

$$m^{(1)}(\mathbf{p}^{vis(1)}, \mathbf{p}^{\chi(1)}, m_{vis}^{(1)}, m_\chi) = m^{(2)}(\mathbf{p}^{vis(2)}, \mathbf{p}^{\chi(2)}, m_{vis}^{(2)}, m_\chi), \tag{101}$$

for the trial momenta given by

$$\begin{aligned} \mathbf{p}^{\chi(1)} &= m_\chi \mathbf{p}^{vis(1)}/m_{vis}^{(1)}, \\ \mathbf{p}^{\chi(2)} &= -\mathbf{p}^{\chi(1)} - \mathbf{p}^{vis(1)} - \mathbf{p}^{vis(2)}, \end{aligned} \tag{102}$$

30

or by

$$
\begin{aligned}
\mathbf{p}^{\chi(2)} &= m_\chi \mathbf{p}^{vis(2)}/m_{vis}^{(2)}, \\
\mathbf{p}^{\chi(1)} &= -\mathbf{p}^{\chi(2)} - \mathbf{p}^{vis(1)} - \mathbf{p}^{vis(2)}.
\end{aligned}
\tag{103}
$$

If some momenta satisfy (101) and (102), or (101) and (103), their back-to-back boost satisfy also the same relations. This means that the boundary is invariant under the back-to-back boost, thus there can not be any crossing of the boundary caused by the back-to-back boost. Therefore, if some visible momenta satisfy (91) or (94), their back-to-back boost satisfy the same condition, so (91) and (94) are covariant under the back-to-back boost (98). The same argument can be used to show that (16) and (19) are covariant under the $(1+2)$-dimensional transformation (27).

In the above, we have argued that m_{I2} is invariant under generic back-to-back Lorentz boost, which leads to

$$
m_{I2}(\mathbf{p}'^{vis(i)}, m_{vis}^{(i)}, m_\chi) = m_{I2}(\mathbf{q}^{vis(i)}, m_{vis}^{(i)}, m_\chi)
\tag{104}
$$

for $\mathbf{q}^{vis(i)}$ obtained by arbitrary back-to-back boost of $\mathbf{p}'^{vis(i)}$. By definition, $\mathbf{p}'^{vis(i)}$ is the i-th visible momentum after the independent longitudinal boosts making the mother particle pair to move back-to-back in the direction of T. One can then choose an appropriate back-to-back boost for which $\mathbf{q}^{vis(i)}$ corresponds to the i-th visible momentum measured in the rest frame of its mother particle.

Let T' denote the transverse plane spanned by $\mathbf{q}^{vis(1)}$ and $\mathbf{q}^{vis(2)}$, and z' denote its normal direction. Then, by definition $q_{z'}^{vis(i)} = 0$, and it is straightforward to minimize $\max\left\{m^{(1)}, m^{(2)}\right\}$ over the z'-component of the trial LSP momentum:

$$
\begin{aligned}
&\min_{\{\mathbf{p}^{\chi(1)}+\mathbf{p}^{\chi(2)}=-\mathbf{q}^{vis(1)}-\mathbf{q}^{vis(2)}\}} \left[\max\left\{m^{(1)}, m^{(2)}\right\}\right] \\
=\ &\min_{\{\mathbf{p}_{T'}^{\chi(1)}+\mathbf{p}_{T'}^{\chi(2)}=-\mathbf{q}_{T'}^{vis(1)}-\mathbf{q}_{T'}^{vis(2)}\}} \left[\max\left\{m^{(1)}, m^{(2)}\right\}_{\mathbf{p}_{z'}^{\chi(1)}=\mathbf{p}_{z'}^{\chi(2)}=0}\right] \\
=\ &\min_{\{\mathbf{p}_{T'}^{\chi(1)}+\mathbf{p}_{T'}^{\chi(2)}=-\mathbf{q}_{T'}^{vis(1)}-\mathbf{q}_{T'}^{vis(2)}\}} \left[\max\left\{m_{T'}^{(1)}, m_{T'}^{(2)}\right\}\right],
\end{aligned}
\tag{105}
$$

and thus

$$
m_{I2}(\mathbf{q}^{vis(i)}, m_{vis}^{(i)}, m_\chi) = m_{T'2}(\mathbf{q}_{T'}^{vis(i)}, m_{vis}^{(i)}, m_\chi).
\tag{106}
$$

Combining (84), (88), (104) and (106), we finally obtain

$$
m_{T2}(\mathbf{p}^{vis(i)}, m_{vis}^{(i)}, m_\chi) \leq m_{T'2}(\mathbf{q}^{vis(i)}, m_{vis}^{(i)}, m_\chi)
\tag{107}
$$

for arbitrary symmetric decay of mother particle pair having a vanishing total transverse momentum in the direction of T, where the equality holds when $T' = T$. Therefore, m_{T2} of any event induced by mother particle pair having a vanishing total transverse momentum in the laboratory frame is *bounded above* by another m_{T2} of an event induced by mother particle pair *at rest*.

Appendix B.

In this appendix, we discuss in detail the m_{T2} of the events associated with the decay of mother particle pair *at rest* with visible momenta in transverse direction. Such m_{T2} corresponds to $m_{T'2}(\mathbf{q}^{vis(i)}, m_{vis}^{(i)}, m_\chi)$, where $\mathbf{q}^{vis(i)}$ denotes the i-th visible momenta measured in the rest frame of its mother particle, and T' is the transverse plane spanned by $\mathbf{q}^{vis(1)}$ and $\mathbf{q}^{vis(2)}$. Since $|\mathbf{q}^{vis(i)}|$ is determined as

$$|\mathbf{q}^{vis(i)}| \;=\; \frac{1}{2\tilde{m}} \left[\left((\tilde{m} + m_{vis}^{(i)})^2 - m_{\tilde{\chi}_1^0}^2 \right) \left((\tilde{m} - m_{vis}^{(i)})^2 - m_{\tilde{\chi}_1^0}^2 \right) \right]^{1/2}, \tag{108}$$

where $\tilde{m}$ is the mother particle mass and $m_{\tilde{\chi}_1^0}$ is the LSP mass, $m_{T'2}$ appears as a function of the three event variables $m_{vis}^{(1)}, m_{vis}^{(2)}, \theta =$ the angle between $\mathbf{q}^{vis(1)}$ and $\mathbf{q}^{vis(2)}$, and also the trial LSP mass m_χ:

$$m_{T'2}(\mathbf{q}^{vis(i)}, m_{vis}^{(i)}, m_\chi) \equiv \mathcal{F}(m_{vis}^{(i)}, \theta, m_\chi). \tag{109}$$

In section 2, we discussed the behavior of $\mathcal{F}$ over the one-dimensional event space with $m_{vis}^{(1)} = m_{vis}^{(2)} = m_{vis}$ and $\theta = 0$. Here we generalize the analysis to the full 3-dimensional event space spanned by $\{m_{vis}^{(i)}, \theta\}$, and show

$$\frac{\partial \mathcal{F}}{\partial \theta} \leq 0 \quad \text{for any } m_{vis}^{(i)}, m_\chi, \text{ and } 0 \leq \theta \leq \pi,$$

$$\left. \frac{\partial \mathcal{F}}{\partial m_{vis}^{(i)}} \right|_{\theta=0} = \begin{cases} \geq 0 & \text{for } m_\chi > m_{\tilde{\chi}_1^0} \text{ and any } m_{vis}^{(i)} \\ \leq 0 & \text{for } m_\chi < m_{\tilde{\chi}_1^0} \text{ and any } m_{vis}^{(i)}, \end{cases} \tag{110}$$

and thus the global maximum of $\mathcal{F}$ over all $\{m_{vis}^{(i)}, \theta\}$ is given by

$$\mathcal{F}^{\max}(m_\chi) = \begin{cases} \mathcal{F}_<^{\max} & \text{for } m_\chi < m_{\tilde{\chi}_1^0} \\ \mathcal{F}_>^{\max} & \text{for } m_\chi > m_{\tilde{\chi}_1^0}, \end{cases} \tag{111}$$

where

$$\begin{aligned} \mathcal{F}_<^{\max} &= \mathcal{F}(m_{vis}^{(1)} = m_{vis}^{\min}, m_{vis}^{(2)} = m_{vis}^{\min}, \theta = 0, m_\chi), \\ \mathcal{F}_>^{\max} &= \mathcal{F}(m_{vis}^{(1)} = m_{vis}^{\max}, m_{vis}^{(2)} = m_{vis}^{\max}, \theta = 0, m_\chi). \end{aligned} \tag{112}$$

As discussed in section 2, m_{T2} is given by either a balanced solution or unbalanced solution, depending upon whether the condition (16) is satisfied or not:

$$\mathcal{F} = \begin{cases} \mathcal{F}^{bal} & \text{for } \mathbf{q}^{vis(i)} \text{ in the balanced domain,} \\ \mathcal{F}^{unbal} & \text{otherwise,} \end{cases}$$

where

$$\left(\mathcal{F}^{\text{bal}}\right)^2 = m_\chi^2 + A \tag{113}$$

$$+ \sqrt{\left(1 + \frac{4m_\chi^2}{2A - (m_{vis}^{(1)})^2 - (m_{vis}^{(2)})^2}\right)\left(A^2 - (m_{vis}^{(1)})^2(m_{vis}^{(2)})^2\right)}, \tag{114}$$

$$\mathcal{F}^{\text{unbal}} = m_\chi + m_{vis}^{(i)} \quad (i = 1 \text{ or } 2) \tag{115}$$

for

$$A = E^{vis(1)}E^{vis(2)} + |\mathbf{q}^{vis(1)}||\mathbf{q}^{vis(2)}|\cos\theta, \tag{116}$$

with $|\mathbf{q}^{vis(i)}|$ given by (108) and $E^{vis(i)} = \sqrt{|\mathbf{q}^{vis(i)}|^2 + (m_{vis}^{(i)})^2}$. Here the balanced domain corresponds to the event set satisfying (16), and $\mathcal{F}^{\text{bal}}$ is obtained from (25) with $\mathbf{p}_T^{vis(i)} = \mathbf{q}^{vis(i)}$. Note that $\mathbf{q}^{vis(i)} = \mathbf{q}_{T'}^{vis(i)}$ and $A = A_{T'}$ according to the definition of T'.

B.1 $\mathcal{F}$ vs. θ

Let us show that $\mathcal{F}$ has its maximum at $\theta = 0$ for given values of $m_{vis}^{(i)}$ and m_χ. If $m_{vis}^{(1)} = m_{vis}^{(2)} \equiv m_{vis}$, one easily finds $\mathcal{F}$ is given by a balanced solution of the form

$$\mathcal{F}^{\text{bal}} = \sqrt{\frac{A + m_{vis}^2}{2}} + \sqrt{\frac{A - m_{vis}^2 + 2m_\chi^2}{2}} \tag{117}$$

which obviously has its maximum at $\theta = 0$ for given values of $m_{vis}^{(i)}$ and m_χ.

To examine the case with $m_{vis}^{(1)} \neq m_{vis}^{(2)}$, let us consider

$$\frac{\partial(\mathcal{F}^{\text{bal}})^2}{\partial\theta} = -\frac{|\mathbf{q}^{vis(1)}||\mathbf{q}^{vis(2)}|\sin\theta}{\sqrt{B^3 C}\chi}\left[(AB - C)\chi^2 + \sqrt{B^3 C}\chi + BC\right], \tag{118}$$

where

$$A \equiv E^{vis(1)}E^{vis(2)} + |\mathbf{q}^{vis(1)}||\mathbf{q}^{vis(2)}|\cos\theta,$$
$$B \equiv 2A - (m_{vis}^{(1)})^2 - (m_{vis}^{(2)})^2,$$
$$C \equiv A^2 - (m_{vis}^{(1)}m_{vis}^{(2)})^2,$$
$$\chi \equiv \sqrt{B + 4m_\chi^2}.$$

It is straightforward to find that $A > 0$, $B > 0$ and $C > 0$ when $m_{vis}^{(1)} \neq m_{vis}^{(2)}$. Then $\mathcal{F}^{\text{bal}}$ has an extremum at $\theta = 0, \pi$ and also at $\theta = \theta_0$ for which

$$\begin{aligned} f &\equiv (AB - C)\chi^2 + \sqrt{B^3 C}\,\chi + BC \\ &= \left((A - (m_{vis}^{(1)})^2)\chi + \sqrt{BC}\right)\left((A - (m_{vis}^{(2)})^2)\chi + \sqrt{BC}\right) = 0, \end{aligned} \tag{119}$$

33

where we have used $AB - C = (A - (m_{vis}^{(1)})^2)(A - (m_{vis}^{(2)})^2)$. Here we will discuss only the case with $m_{vis}^{(1)} > m_{vis}^{(2)}$ since the result for $m_{vis}^{(1)} < m_{vis}^{(2)}$ can be obtained by interchanging $m_{vis}^{(1)}$ and $m_{vis}^{(2)}$.

If $AB - C \geq 0$, $f > 0$ for $\chi \geq 0$, and thus

$$\frac{\partial \mathcal{F}^{\text{bal}}}{\partial \theta} \leq 0 \quad \text{for any } m_{vis}^{(i)}, \theta, m_\chi \text{ with } AB - C \geq 0. \tag{120}$$

As $\mathcal{F}^{\text{unbal}} = m_\chi + m_{vis}^{(1)}$ is independent of θ, this means that $\partial \mathcal{F}/\partial \theta \leq 0$, thus $\mathcal{F}$ has its maximum at $\theta = 0$ for $m_{vis}^{(i)}, m_\chi$ giving $AB - C \geq 0$.

In other case with $AB - C < 0$, one finds $f \geq 0$ for $0 < \chi \leq \chi_0$, while $f < 0$ for $\chi > \chi_0$, where

$$\chi_0 = \frac{\sqrt{BC}}{(m_{vis}^{(1)})^2 - A}. \tag{121}$$

Since θ_0 corresponds to the value of θ for which $\chi = \chi_0$ (for given values of $m_{vis}^{(i)}$ and m_χ), this implies

$$f = \begin{cases} \geq 0 & \text{for } 0 < \theta \leq \theta_0, \\ < 0 & \text{for } \theta_0 < \theta < \pi, \end{cases} \tag{122}$$

and thus $\mathcal{F}^{\text{bal}}$ decreases as θ varies from zero to θ_0, while it increases as θ varies from θ_0 to π. On the other hand, $\chi \equiv \sqrt{B + 4m_\chi^2} = \chi_0$ leads to

$$A\big|_{\theta=\theta_0} = \frac{m_{vis}^{(1)}\left(2m_{vis}^{(1)}m_\chi + (m_{vis}^{(1)})^2 + (m_{vis}^{(2)})^2\right)}{2(m_\chi + m_{vis}^{(1)})} \tag{123}$$

for which

$$\mathcal{F}^{\text{bal}}\big|_{\theta=\theta_0} = m_\chi + m_{vis}^{(1)} = \mathcal{F}^{\text{unbal}}. \tag{124}$$

This means that $\theta = \theta_0$ corresponds to the boundary between the balanced domain and the unbalanced domain. One can show also $\mathcal{F}^{\text{bal}} \geq \mathcal{F}^{\text{unbal}}$ for $\theta \geq \theta_0$, where the equality holds for $\theta = \theta_0$, implying that $\mathcal{F}$ is given by $\mathcal{F}^{\text{unbal}}$ for $\theta_0 < \theta \leq \pi$, while it is given by $\mathcal{F}^{\text{bal}}$ for $0 \leq \theta \leq \theta_0$. Again, combined with that $\mathcal{F}^{\text{unbal}}$ is independent of θ, these observations lead to

$$\frac{\partial \mathcal{F}}{\partial \theta} \leq 0 \quad \text{for } AB - C < 0, \tag{125}$$

thus $\mathcal{F}$ has its maximum at $\theta = 0$ for $m_{vis}^{(i)}, m_\chi$ giving $AB - C < 0$ also.

B.2 $\mathcal{F}$ vs. $m_{vis}^{(i)}$:

Let us now examine the dependence of $\mathcal{F}$ on $m_{vis}^{(i)}$. As we are interested in the events giving $\mathcal{F}^{\max}$, we will fix $\theta = 0$ in the following. We then have

$$\frac{\partial(\mathcal{F}^{\text{bal}})^2}{\partial(m_{vis}^{(1)})^2} = \frac{g}{2\sqrt{B^3 C}\chi}, \tag{126}$$

where

$$g \equiv (BC' - B'C)\chi^2 + \sqrt{B^3 C}(B' + 1)\chi + B'BC \tag{127}$$

with

$$A' \equiv \frac{\partial A}{\partial(m_{vis}^{(1)})^2}, \quad B' \equiv \frac{\partial B}{\partial(m_{vis}^{(1)})^2}, \quad C' \equiv \frac{\partial C}{\partial(m_{vis}^{(1)})^2}. \tag{128}$$

The equation $g = 0$ can have the following solutions:

$$\begin{aligned}
\chi_1 &= \frac{\sqrt{BC}(1 - 2A')}{2A'(A - (m_{vis}^{(1)})^2) + A - (m_{vis}^{(2)})^2}, \\
\chi_2 &= \frac{\sqrt{BC}}{(m_{vis}^{(2)})^2 - A},
\end{aligned} \tag{129}$$

where we have used

$$BC' - B'C = (A - (m_{vis}^{(2)})^2)\left(2A'(A - (m_{vis}^{(1)})^2) + A - (m_{vis}^{(2)})^2\right)$$

and

$$\left((m_{vis}^{(1)})^2 - (m_{vis}^{(2)})^2\right)A' - A + (m_{vis}^{(2)})^2 < 0 \quad \text{for } m_{vis}^{(1)} \neq m_{vis}^{(2)}.$$

If $m_{vis}^{(1)} \neq m_{vis}^{(2)}$, we have also

$$\begin{aligned}
B' &= (2A' - 1) < 0, \\
2A'(A - (m_{vis}^{(1)})^2) + A - (m_{vis}^{(2)})^2 &> 0,
\end{aligned} \tag{130}$$

and thus χ_1 is always positive, while the sign of χ_2 is determined by the sign of $A - (m_{vis}^{(2)})^2$.
If $m_{vis}^{(1)} > m_{vis}^{(2)}$, we have $\mathcal{F}^{\text{unbal}} = m_\chi + m_{vis}^{(1)}$, and thus

$$\frac{\partial \mathcal{F}^{\text{unbal}}}{\partial m_{vis}^{(1)}} = 1 \quad \text{for } m_{vis}^{(1)} > m_{vis}^{(2)}. \tag{131}$$

As for the behavior of $\mathcal{F}^{\rm bal}$, since $A - (m_{vis}^{(2)})^2 > 0$ for $m_{vis}^{(1)} > m_{vis}^{(2)}$, only $\chi = \chi_1$ can be a physical solution of $g = 0$, for which

$$\sqrt{B + 4m_\chi^2} = \frac{\sqrt{BC}(1 - 2A')}{2A'(A - (m_{vis}^{(1)})^2) + A - (m_{vis}^{(2)})^2}. \tag{132}$$

This equation is solved by $m_\chi = m_{\tilde{\chi}_1^0}$, which means $g = 0$ at $m_\chi = m_{\tilde{\chi}_1^0}$. It is also straightforward to find that $g > 0$ for $m_\chi > m_{\tilde{\chi}_1^0}$ and $g < 0$ for $m_\chi < m_{\tilde{\chi}_1^0}$, leading to

$$\frac{\partial \mathcal{F}^{\rm bal}}{\partial m_{vis}^{(1)}} = \begin{cases} \leq 0 & \text{for } m_\chi < m_{\tilde{\chi}_1^0} \text{ and } m_{vis}^{(1)} > m_{vis}^{(2)}, \\ \geq 0 & \text{for } m_\chi > m_{\tilde{\chi}_1^0} \text{ and } m_{vis}^{(1)} > m_{vis}^{(2)}. \end{cases} \tag{133}$$

On the other hand, if $m_\chi < m_{\tilde{\chi}_1^0}$ and $\theta = 0$, $\mathcal{F}$ is always given by $\mathcal{F}^{\rm bal}$. We then find from (131) and (133) that

$$\frac{\partial \mathcal{F}}{\partial m_{vis}^{(1)}} = \begin{cases} \leq 0 & \text{for } m_\chi < m_{\tilde{\chi}_1^0} \text{ and } m_{vis}^{(1)} > m_{vis}^{(2)}, \\ \geq 0 & \text{for } m_\chi > m_{\tilde{\chi}_1^0} \text{ and } m_{vis}^{(1)} > m_{vis}^{(2)}. \end{cases} \tag{134}$$

In other case with $m_{vis}^{(1)} < m_{vis}^{(2)}$, we have $\mathcal{F}^{\rm unbal} = m_\chi + m_{vis}^{(2)}$, so

$$\frac{\partial \mathcal{F}^{\rm unbal}}{\partial m_{vis}^{(1)}} = 0 \quad \text{for } m_{vis}^{(1)} < m_{vis}^{(2)}. \tag{135}$$

In this case, $A - (m_{vis}^{(2)})^2$ can be either positive or negative. If it is positive, again $\chi = \chi_1$ is the only solution for $g = 0$. Then, one can repeat the analysis leading to (133), and find

$$\frac{\partial \mathcal{F}}{\partial m_{vis}^{(1)}} = \begin{cases} \leq 0 & \text{for } m_\chi < m_{\tilde{\chi}_1^0}, \ m_{vis}^{(1)} < m_{vis}^{(2)}, \ A - (m_{vis}^{(2)})^2 > 0 \\ \geq 0 & \text{for } m_\chi > m_{\tilde{\chi}_1^0}, \ m_{vis}^{(1)} < m_{vis}^{(2)}, \ A - (m_{vis}^{(2)})^2 > 0 \end{cases} \tag{136}$$

However, if $A - (m_{vis}^{(2)})^2 < 0$, both $\chi = \chi_1$ and $\chi = \chi_2$ become a good solution of $g = 0$, and $\chi_2 > \chi_1$. Again, $\chi = \chi_1$ is obtained if and only if $m_\chi = m_{\tilde{\chi}_1^0}$. As for the other solution $\chi = \chi_2$, i.e.

$$\sqrt{B + 4m_\chi^2} = \frac{\sqrt{BC}}{(m_{vis}^{(2)})^2 - A}, \tag{137}$$

it is straightforward to find that it gives rise to

$$\mathcal{F}^{\rm bal}\Big|_{\chi=\chi_2} = m_\chi + m_{vis}^{(2)} = \mathcal{F}^{\rm unbal}, \tag{138}$$

which means that $\chi = \chi_2$ corresponds to the boundary between the balanced domain and the unbalanced domain. In Fig. 13, we depict the 2-dimensional event space of $(m_{vis}^{(1)}, m_{vis}^{(2)})$

36

for $\theta = 0$ and $m_\chi > m_{\tilde{\chi}_1^0}$, showing the balanced domain (B) and the unbalanced domain (UB).

The above observation implies that $\mathcal{F}$ is always given by $\mathcal{F}^{\text{bal}}$ if $\chi < \chi_1$, for which $m_\chi < m_{\tilde{\chi}_1^0}$. One can show that $g < 0$ in such case, so

$$\frac{\partial \mathcal{F}}{\partial m_{vis}^{(1)}} \leq 0 \quad \text{for } m_\chi < m_{\tilde{\chi}_1^0}, \ m_{vis}^{(1)} < m_{vis}^{(2)}, \ A - (m_{vis}^{(2)})^2 < 0. \tag{139}$$

However, if $\chi \geq \chi_1$, for which $m_\chi \geq m_{\tilde{\chi}_1^0}$, the function g can have either sign. We find that $g \geq 0$ for $\chi_1 \leq \chi \leq \chi_2$, while $g \leq 0$ for $\chi \geq \chi_2$. As $\chi = \chi_2$ corresponds to the boundary between the balanced domain and the unbalanced domain, this means that $g \geq 0$ when $\mathcal{F}$ is given by $\mathcal{F}^{\text{bal}}$, so

$$\frac{\partial \mathcal{F}}{\partial m_{vis}^{(1)}} = \frac{\partial \mathcal{F}^{\text{bal}}}{\partial m_{vis}^{(1)}} \geq 0$$

$$\text{for } m_\chi > m_{\tilde{\chi}_1^0}, \ m_{vis}^{(1)} < m_{vis}^{(2)}, \ A - (m_{vis}^{(2)})^2 < 0, \ \chi_1 \leq \chi \leq \chi_2. \tag{140}$$

If $\chi \geq \chi_2$ with $m_{vis}^{(1)} < m_{vis}^{(2)}$, $\mathcal{F}$ is given by $\mathcal{F}^{\text{unbal}} = m_\chi + m_{vis}^{(2)}$, so

$$\frac{\partial \mathcal{F}}{\partial m_{vis}^{(1)}} = \frac{\partial \mathcal{F}^{\text{unbal}}}{\partial m_{vis}^{(1)}} = 0$$

$$\text{for } m_\chi > m_{\tilde{\chi}_1^0}, \ m_{vis}^{(1)} < m_{vis}^{(2)}, \ A - (m_{vis}^{(2)})^2 < 0, \ \chi \geq \chi_2. \tag{141}$$

Combining all of the above results together, and also taking into account that $\mathcal{F}$ is invariant under the exchange of $m_{vis}^{(1)}$ and $m_{vis}^{(2)}$, we finally obtain

$$\left. \frac{\partial \mathcal{F}}{\partial m_{vis}^{(i)}} \right|_{\theta=0} = \begin{cases} \leq 0 & \text{for } m_\chi < m_{\tilde{\chi}_1^0} \text{ and any } m_{vis}^{(i)} \\ \geq 0 & \text{for } m_\chi > m_{\tilde{\chi}_1^0} \text{ and any } m_{vis}^{(i)}. \end{cases} \tag{142}$$

In Fig.(14), we depict the pattern of the 2-d vector field $\partial \mathcal{F}/\partial m_{vis}^{(i)}$ for both cases with $m_\chi < m_{\tilde{\chi}_1^0} \ (\chi < \chi_1)$ and $m_\chi > m_{\tilde{\chi}_1^0} \ (\chi > \chi_2)$, showing the above result explicitly. Together with the observation that $\mathcal{F}$ has its maximum at $\theta = 0$ for given values of $m_{vis}^{(i)}$ and m_χ, the above result assures that the global maximum of the m_{T2} function $\mathcal{F}$ over the 3-dimensional event space parameterized by $\{m_{vis}^{(i)}, \theta\}$ is given by

$$\mathcal{F}^{\text{max}}(m_\chi) = \begin{cases} \mathcal{F}_<^{\text{max}} & \text{for } m_\chi < m_{\tilde{\chi}_1^0} \\ \mathcal{F}_>^{\text{max}} & \text{for } m_\chi > m_{\tilde{\chi}_1^0}, \end{cases} \tag{143}$$

where

$$\begin{aligned} \mathcal{F}_<^{\text{max}} &= \mathcal{F}(m_{vis}^{(1)} = m_{vis}^{\text{min}}, m_{vis}^{(2)} = m_{vis}^{\text{min}}, \theta = 0, m_\chi), \\ \mathcal{F}_>^{\text{max}} &= \mathcal{F}(m_{vis}^{(1)} = m_{vis}^{\text{max}}, m_{vis}^{(2)} = m_{vis}^{\text{max}}, \theta = 0, m_\chi). \end{aligned} \tag{144}$$
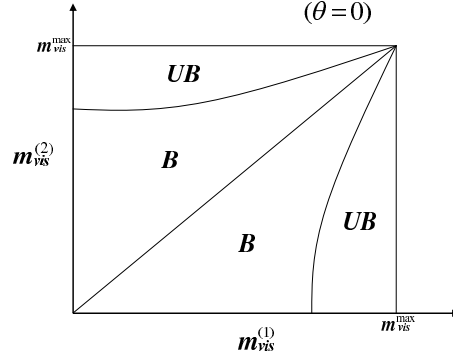
Figure 13: Division of the $(m_{vis}^{(1)}, m_{vis}^{(2)})$ into the balanced solution region (B) and the unbalanced region (UB).
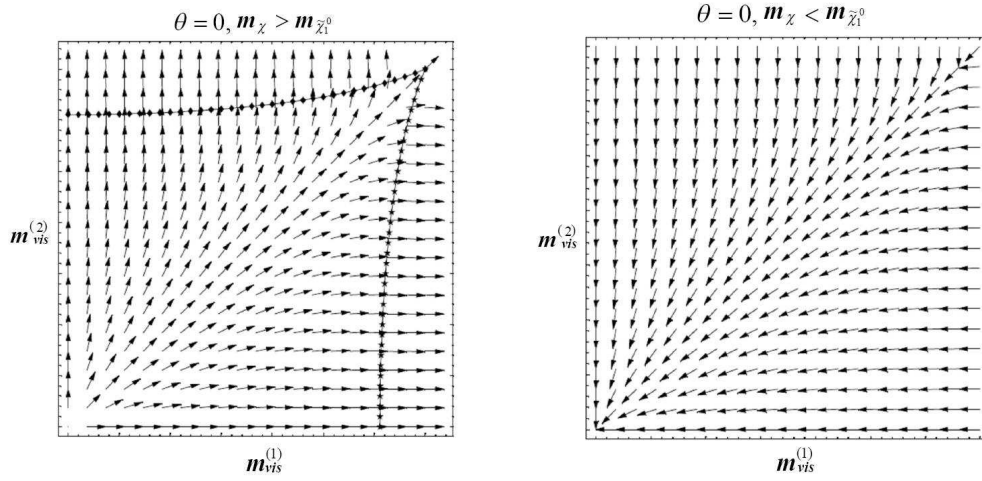

Figure 14: The gradient of $\mathcal{F}$ for (a) $m_\chi > m_{\tilde{\chi}_1^0}$ and $\theta = 0$, (b) $m_\chi < m_{\tilde{\chi}_1^0}$ and $\theta = 0$.

References

[1] ATLAS Technical Proposal, CERN-LHCC-94-43.

[2] CMS Physics Technical Design Report, CERN-LHCC-2006-021.

[3] H. P. Nilles, Phys. Rept. **110** (1984) 1; H. E. Haber and G. L. Kane, Phys. Rept. **117** (1985) 75.

[4] G. Weiglein *et al.*, [LHC/LC Study Group], Phys. Rept. **426** (2006) 47.

[5] K. Choi and H. P. Nilles, JHEP **0704** (2007) 006.

[6] W.S. Cho, K. Choi, Y.G. Kim, and C.B.Park, arXiv:0709.0288 [hep-ph].

[7] B. Gripaios, arXiv:0709.2740 [hep-ph].

[8] A.J. Barr, B. Gripaios and C.G. Lester, arXiv:0711.4008 [hep-ph].

[9] I. Hinchliffe, F. E. Paige, M. D. Shapiro, J. Soderqvist and W. Yao, Phys. Rev. D **55**, 5520 (1997) [hep-ph/9610544]; H. Bachacou, I. Hinchliffe, F. E. Paige (Brookhaven), Phys. Rev. D **62**, 015009 (2000) [hep-ph/9907518].

[10] B. C. Allanach, C. G. Lester, M. A. Parker and B. R. Webber, JHEP **0009**, 004 (2000) [hep-ph/0007009]; K. Kawagoe, M. M. Nojiri and G. Polesello, Phys. Rev. D **71**, 035008 (2005) [hep-ph/0410160]; B. K. Gjelsten, D. J. Miller and P. Osland, JHEP **0506**, 015 (2005) [hep-ph/0501033].

[11] H.-C. Cheng, J. F. Gunion, Z. Han, G. Marandella and B. McElrath, arXiv:0707.0030 [hep-ph].

[12] V. D. Barger, A. D. Martin, and R. J. N. Phillips, Z. Phys. **C 21** (1983) 99.

[13] C. G. Lester and D. J. Summers, Phys. Lett. **B 463** (1999) 99-103.

[14] A. Barr, C. G. Lester, and Phil Stephens, J.Phys.G29:2343-2363,2003.

[15] C. Lester and A. Barr, arXiv:0708.1028.

[16] K. Choi, A. Falkowski, H. P. Nilles, M. Olechowski and S. Pokorski, JHEP **0411**, 076 (2004) [hep-th/0411066]; K. Choi, A. Falkowski, H. P. Nilles and M. Olechowski, Nucl. Phys. **B718** (2005) 113 [hep-th/0503216]; K. Choi, K. S. Jeong and K. i. Okumura, JHEP **0509**, 039 (2005) [arXiv:hep-ph/0504037]; M. Endo, M. Yamaguchi and K. Yoshioka, Phys. Rev. D**72**, 015004 (2005) [hep-ph/0504036]; A. Falkowski, O. Lebedev, Y. Mambrini, JHEP **0511**, 034 (2005) [hep-ph/0507110].

[17] T. Sjostrand, P. Eden, C. Friberg, L. Lonnblad, G. Miu, S. Mrenna and E. Norrbin, Computer Physics Commun. 135 (2001) 238; T. Sjostrand, S. Mrenna and P. Skands, LU TP 06-13, FERMILAB-PUB-06-052-CD-T [hep-ph/0603175].

[18] http://twiki.cern.ch/twiki/bin/view/Atlas/StransverseMassLibrary.

[19] L. Randall and R. Sundrum, Nucl. Phys. **B 557** (1999) 79 [hep-th/9810155]; G. F. Giudice, M. A. Luty, H. Murayama and R. Rattazzi, JHEP **12** (1998) 027 [hep-ph/9810442].

[20] http://www.physics.ucdavis.edu/∼conway/research/software/pgs/pgs4-general.htm.

[21] http://twiki.cern.ch/twiki/bin/view/CMS/SusyAnalyzer.

[22] B.C. Allanach *et al.*, Eur. Phys. J. C **25** (2002) 113 [hep-ph/0202233].